PROCEEDINGS A

royalsocietypublishing.org/journal/rspa

Research

Cite this article: Laing CR, Krauskopf B. 2025 Periodic solutions for a pair of delay-coupled excitable theta neurons. *Proc. R. Soc. A* **481**: 20240897.
https://doi.org/10.1098/rspa.2024.0897

Received: 20 November 2024
Accepted: 23 April 2025

Subject Areas:
applied mathematics

Keywords:
neuron dynamics, self-pulsations, delay differential equations, bifurcation analysis

Author for correspondence:
Carlo R. Laing
e-mail: c.r.laing@massey.ac.nz

Periodic solutions for a pair of delay-coupled excitable theta neurons

Carlo R. Laing[1] and Bernd Krauskopf[2]

[1]School of Mathematical and Computational Sciences, Massey University, Private Bag 102-904, North Shore Mail Centre, Auckland 0745, New Zealand
[2]Department of Mathematics, The University of Auckland, Private Bag 92019, Auckland 1142, New Zealand

CRL, 0000-0002-6086-2978; BK, 0000-0002-8940-230X

We consider a pair of identical theta neurons in the excitable regime, each coupled to the other via a delayed Dirac delta function with the same delay. This simple network can support different periodic solutions, and we concentrate on two important types: those for which the neurons are perfectly synchronous, and those where the neurons are exactly half a period out of phase and fire alternatingly. Owing to the specific type of pulsatile feedback, we are able to determine these solutions and their stability analytically. More specifically, (infinitely many) branches of periodic solutions of either type are created at saddle-node bifurcations, and they gain stability at symmetry-breaking bifurcations when their period as a function of the delay is at its minimum. We also determine the respective branches of symmetry-broken periodic solutions and show that they are all unstable. We demonstrate by considering smoothed pulse-like coupling that the special case of the Dirac delta function can be seen as a sort of normal form: the basic structure of the different periodic solutions of the two theta neurons is preserved, but there may be additional changes of stability along the different branches.

1. Introduction

Excitability is a common phenomenon in nonlinear dynamical systems [1,2]. An excitable system typically

THE ROYAL SOCIETY PUBLISHING

has a stable resting state and, when subject to a small perturbation, stays near and relaxes to this resting state. However, for a sufficiently large perturbation above what is known as the *excitability threshold*, the system has a stereotypical response (such as a neuron firing an action potential or a laser emitting a pulse of light) before returning to the rest state; here, the magnitude of the response is largely independent of the size of the perturbation, once it is above the excitability threshold.

We consider here the prototypical example known as the *theta neuron*, which is a mathematical model for the single angular variable $\theta(t) \in (-\pi, \pi]$, given by

$$\frac{\mathrm{d}\theta}{\mathrm{d}t} = 1 - \cos\theta + (1 + \cos\theta)I. \tag{1.1}$$

The theta neuron is the normal form of the saddle-node-on-invariant-circle bifurcation [3,4] and has the advantage that its dynamics can be found explicitly for constant I. In particular, this system is excitable when $I < 0$, in which case it has two equilibria at $\theta_\pm = \pm 2\tan^{-1}(\sqrt{-I})$, where θ_- is the stable rest state and θ_+ is unstable and forms the excitability threshold. A perturbation applied at θ_- that moves θ above θ_+ results in θ moving through π before returning to θ_-, and (by convention) this is the moment when the theta neuron 'fires' and produces a pulse. Note that, under the transformation $V = \tan(\theta/2)$, the theta neuron is equivalent to the quadratic integrate-and-fire neuron with the rule $V(t^+) = -\infty$ if $V(t^-) = \infty$, i.e. V is reset when the neuron fires.

An excitable unit, such as a neuron cell or excitable optical element, is able to react to inputs with the generation of a pulse, depending on the strength and timing of the inputs. Whenever a number of neurons or other elements are coupled to themselves and/or to each other, there are necessarily delays in when they receive input and how fast they react to it [5]. Such delays may play an important role and, more generally, they are ubiquitous in dynamical systems. In particular, it is of interest to study the behaviour of excitable systems with delayed interactions, where delays range from synaptic processing delays in neural systems [6] to delays between coupled optical systems, which arise even when signals travel at the speed of light [7].

In our previous work [8], we studied a single theta neuron with delayed self-coupling given by a Dirac delta function of time. This specific type of pulsatile feedback allows us to analytically determine the dynamics between times at which the feedback acts, which can be described equivalently by a discrete map for the spike times. This allowed us to find explicit expressions for all periodic solutions, their stability and bifurcations of this excitable system with self-feedback. Our results show that the theta neuron with delayed delta function self-coupling can be considered as a sort of normal form: while being fully treatable analytically, it captures the essentials of observed self-sustained oscillations in excitable systems with delayed self-feedback, including laser systems [7,9–13] and an actual cell [14].

In this paper, we consider two identical theta neurons that are delay-coupled via Dirac delta functions to one another. To this end, we set $I = -1$ from now on without loss of generality (see appendix B) and study the system

$$\frac{\mathrm{d}\theta_1}{\mathrm{d}t} = 1 - \cos\theta_1 + (1 + \cos\theta_1)\left(-1 + \kappa \sum_{i:t-\tau<s_i<t} \delta(t - s_i - \tau)\right) \tag{1.2}$$

and

$$\frac{\mathrm{d}\theta_2}{\mathrm{d}t} = 1 - \cos\theta_2 + (1 + \cos\theta_2)\left(-1 + \kappa \sum_{i:t-\tau<t_i<t} \delta(t - t_i - \tau)\right). \tag{1.3}$$

Here, τ is the (constant) delay and κ is the strength of coupling between the neurons, the firing times in the past of neuron 1 are $\{\ldots, t_{-3}, t_{-2}, t_{-1}, t_0\}$ and those of neuron 2 are

royalsocietypublishing.org/journal/rspa Proc. R. Soc. A 481: 20240897

$\{\ldots, s_{-3}, s_{-2}, s_{-1}, s_0\}$. Moreover, the influence of the delta function is to increment θ according to

$$\tan\left(\frac{\theta^+}{2}\right) = \tan\left(\frac{\theta^-}{2}\right) + \kappa, \tag{1.4}$$

where θ^- and θ^+ are the values of θ before and after the delta function acts, respectively [8].

The system of equations (1.2)–(1.3) constitute the next step up in complexity from the case of a delay-self-coupled theta neuron studied in [8] and, at the same time, it is a normal form for the simplest case of a network of only two delay-coupled excitable cells or elements. Pairs of oscillators of different type with delayed coupling have been studied commonly [15–17]. The case of two delay-coupled excitable cells or elements, however, appears to have received less attention. We now discuss previous work on oscillations in such a system, which mostly concerns delay-coupled FitzHugh–Nagumo (FHN) systems. In [18,19] two FHN systems with diffusive delay-coupling are considered. A stable periodic solution is found, where the individual FHN systems oscillate out of phase with one another, with a period slightly greater than twice the delay; this solution disappears in a saddle-node bifurcation as the delay is decreased. A pair of delay-coupled FHN systems is studied in [20], and in-phase and anti-phase periodic solutions are found, albeit for a parameter regime where the uncoupled FHN systems have periodic solutions, rather than being excitable. Both in-phase and anti-phase periodic solutions, with periods approximately equal to the delay and twice the delay, respectively, are also found in [21] for a pair of modified FHN systems. Two delay-coupled excitable FHN systems are studied in [22], where both synchronous and alternating period solutions are found and the existence of less-symmetric periodic solutions is also mentioned. A living coupled oscillator system is constructed in [23] by using a plasmodial slime mould; depending on (effectively) the delay and the coupling strength between the two subparts, both synchronous and alternating periodic solutions are found.

We show here that our approach and techniques can be used to find all periodic solutions of equations (1.2)–(1.3), which may have differing spatio-temporal symmetries in light of the symmetry of exchanging the two theta neurons. Explicit expressions for $\theta_{1,2}$ between the times at which the delta function acts, in conjunction with the effect of the delta function coupling equation (1.4), allow us to construct these periodic solutions. More specifically, we derive a map for the next firing times and linearize it about a periodic solution to obtain analytic expressions for its stability. This technique is similar to that in [24], with the main difference being that they consider oscillators for which $\mathrm{d}\theta/\mathrm{d}t$ is constant between the times at which the coupling acts, so that when uncoupled an oscillator will fire periodically. By contrast, the excitable neurons we consider will fire at most once when uncoupled. We also mention in this context the work of [25], who consider a network of three-phase oscillators coupled by delayed Dirac delta functions.

The paper is structured as follows. We analyse synchronous (in-phase) periodic solutions in §2, where we determine conditions for their existence and stability, and also describe symmetry-broken solutions that branch from them. In §3, we perform a similar analysis for alternating (anti-phase) periodic solutions for which the neurons fire half a period out of phase with one another. A numerical bifurcation study in §4 shows that the basic structure of the different periodic solutions is preserved when the delayed coupling is smooth rather than given by a delta function; however, there may be additional changes of stability along branches of periodic solutions. We conclude in §5, where we also briefly mention directions for future research. In the appendix we present arguments to establish the instability of the symmetry-broken solutions that bifurcate from the synchronous and the alternating periodic solutions, as well as the rescaling of negative I to -1.

2. Synchronous solutions

Since we set $I = -1$, each individual theta neuron, as described by equation (1.1) with variable θ (standing for θ_1 and/or θ_2) has its equilibria at $\theta_\pm = \pm\pi/2$. If an initial condition $\theta(0)$ satisfies

royalsocietypublishing.org/journal/rspa Proc. R. Soc. A 481: 20240897

$\theta_+ = \pi/2 < \theta(0)$ then the solution of equation (1.1) (with $I = -1$) is

$$\theta(t) = 2\tan^{-1}\left[-\coth\left(t - \coth^{-1}\left[\tan\left(\frac{\theta(0)}{2}\right)\right]\right)\right]. \tag{2.1}$$

For our analysis in this and the next section, we need two special cases of this explicit solution. If the neuron has fired at $t = 0$, i.e. $\theta(0) = \pi$, then

$$\theta(t) = 2\tan^{-1}\left[-\coth(t)\right], \tag{2.2}$$

where t is the time since firing. Moreover, when $\theta(0) > \pi/2$, the time Δ until firing satisfies

$$\pi = 2\tan^{-1}\left[-\coth\left(\Delta - \coth^{-1}\left[\tan\left(\frac{\theta(0)}{2}\right)\right]\right)\right],$$

which reduces to

$$\Delta = \coth^{-1}\left[\tan\left(\frac{\theta(0)}{2}\right)\right]. \tag{2.3}$$

An important property of equations (1.2)–(1.3) is its reflection symmetry of interchanging the two theta neurons, given formally by $(\theta_1, \theta_2) \mapsto (\theta_2, \theta_1)$. General theory [26] implies the possibility of periodic solutions with different spatio-temporal symmetries, including those where the two neuron are in phase, in anti-phase, or have an intermediate phase between them. Note also that the solution $\theta_1 = \theta_2 = 3\pi/2$ is a stable fixed point of equations (1.2)–(1.3) for any κ. Thus, to observe periodic solutions, there must have been some firing of at least one of the neurons in the past (for example, due to an external stimulus).

In this section, we consider the first type of periodic solution of equations (1.2)–(1.3), where the neurons are in phase, i.e. they are perfectly synchronous. The influence of one neuron on the other is then the same as that of the neuron on itself. While the existence of such synchronous solutions is governed by the equations of a single neuron with delayed self-coupled [8], their stability is more complicated. That is, there is now the possibility of bifurcations out of the symmetry subspace (where the two phases are equal), which creates solutions for which the neurons have a phase difference and are, hence, no longer perfectly synchronized. The results in this section are summarized by figure 1, which shows the branches of synchronous periodic solutions, their stability and bifurcations, as well as branches of bifurcating symmetry-broken periodic solutions.

(a) Existence and stability of synchronous periodic solutions

As shown in [8], perfectly synchronous periodic solutions of equations (1.2)–(1.3) with period T satisfy

$$\coth\left[(n+1)T - \tau\right] = \kappa + \coth\left[nT - \tau\right], \tag{2.4}$$

where n is the number of past firing times in the interval $(-\tau, 0)$, assuming that a neuron has just fired at time $t = 0$, and $\kappa > 2$. The primary branch, corresponding to $n = 0$, is given explicitly by

$$T(\tau) = \tau + \coth^{-1}(\kappa - \coth\tau). \tag{2.5}$$

Secondary branches are given parametrically, by using the reappearance of periodic solutions in delay differential equations (DDEs) with fixed delays [27], as

$$(\tau, T) = (s + nT(s), T(s)), \tag{2.6}$$

where $\coth^{-1}(\kappa - 1) < s < \infty$.

These branches of synchronous periodic solutions are shown in figure 1 for $n = 0, 1, 2, 3, 4$ and $\kappa = 5$: they are the tilted parabola shaped curves that are also shown in [8, fig. 3] for the case of a single theta neuron. However, the stability of the periodic solutions is different for the case of two synchronous theta neurons, and this is seen as follows.

Suppose neuron 1 last fired at time t_0 and neuron 2 last fired at s_0 where $s_0 \approx t_0$. The most distant past firing of neuron 1 in $(t_0 - \tau, t_0)$ is t_{-n} and the most distant past firing of neuron 2 in

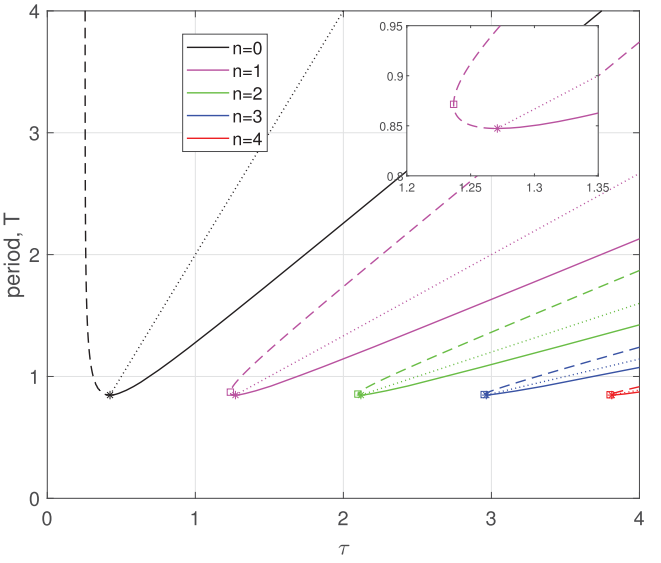

Figure 1. Branches of synchronous and corresponding symmetry-broken periodic solutions of equations (1.2)–(1.3) with $n = 0, 1, 2, 3, 4$. Solid curves are stable (to the right of each minimum) and dashed curves are unstable. Saddle-node bifurcations are marked with squares, symmetry-breaking bifurcations with stars and bifurcating pairs of symmetry-broken solutions are represented by dotted lines. The inset is an enlargement of the branch with $n = 1$. Here, $\kappa = 5$. Note that continuation of the saddle-node bifurcations in the (τ, κ)-plane is shown in fig. 5 of [8].

$(s_0 - \tau, s_0)$ is s_{-n}. After t_0, neuron 1 has its phase incremented for the next time at $\tau - (t_0 - s_{-n})$ due to a past firing of neuron 2. Before the reset, from equation (2.2), θ_1 equals

$$\theta_1^- = 2\tan^{-1}\left[-\coth\left(\tau - (t_0 - s_{-n})\right)\right]$$

and after reset it is θ_1^+, where

$$\tan\left(\frac{\theta_1^+}{2}\right) = \tan\left(\frac{\theta_1^-}{2}\right) + \kappa.$$

Neuron 1 will then fire after a further time Δ_1 where, from equation (2.3),

$$\Delta_1 = \coth^{-1}\left[\tan\left(\frac{\theta_1^+}{2}\right)\right].$$

Thus, we conclude that $t_1 = t_0 + \tau - (t_0 - s_{-n}) + \Delta_1$.

The argument for neuron 2 is the same: its phase is incremented for the first time at $\tau - (s_0 - t_{-n})$, and the analogous expressions for θ_2^- and θ_2^+ mean that neuron 2 will then fire after the further time

$$\Delta_2 = \coth^{-1}\left[\tan\left(\frac{\theta_2^+}{2}\right)\right],$$

yielding $s_1 = s_0 + \tau - (s_0 - t_{-n}) + \Delta_2$.

Hence, we have

$$s_1 = \tau + t_{-n} + \coth^{-1}\left[\tan\left(\frac{\theta_2^-}{2}\right) + \kappa\right] = \tau + t_{-n} + \coth^{-1}\left[\kappa - \coth\left(\tau - s_0 + t_{-n}\right)\right]$$

and

$$t_1 = \tau + s_{-n} + \coth^{-1}\left[\tan\left(\frac{\theta_1^-}{2}\right) + \kappa\right] = \tau + s_{-n} + \coth^{-1}\left[\kappa - \coth\left(\tau - t_0 + s_{-n}\right)\right],$$

royalsocietypublishing.org/journal/rspa Proc. R. Soc. A 481: 20240897

which give s_1 and t_1 in terms of previous firing times. By considering this argument for different i, we obtain the general case

$$s_{i+1} = \tau + t_{i-n} + \coth^{-1}\left[\kappa - \coth\left(\tau - s_i + t_{i-n}\right)\right] \tag{2.7}$$

and

$$t_{i+1} = \tau + s_{i-n} + \coth^{-1}\left[\kappa - \coth\left(\tau - t_i + s_{i-n}\right)\right], \tag{2.8}$$

which we write in the form

$$F(s_{i+1}, t_{i-n}, s_i) = 0$$

and

$$G(t_{i+1}, s_{i-n}, t_i) = 0.$$

To determine stability, we perturb $t_i \to t_i + \eta_i$ and $s_i \to s_i + \mu_i$, which gives to linear order

$$\frac{\partial F}{\partial s_{i+1}}\mu_{i+1} + \frac{\partial F}{\partial t_{i-n}}\eta_{i-n} + \frac{\partial F}{\partial s_i}\mu_i = 0 \tag{2.9}$$

and

$$\frac{\partial G}{\partial t_{i+1}}\eta_{i+1} + \frac{\partial G}{\partial s_{i-n}}\mu_{i-n} + \frac{\partial G}{\partial t_i}\eta_i = 0. \tag{2.10}$$

When evaluating the partial derivatives at a periodic solution with period T, this becomes

$$-\mu_{i+1} + (1-\gamma)\eta_{i-n} + \gamma\mu_i = 0 \tag{2.11}$$

and

$$-\eta_{i+1} + (1-\gamma)\mu_{i-n} + \gamma\eta_i = 0, \tag{2.12}$$

where

$$\gamma = \frac{\coth^2(\tau - nT) - 1}{[\kappa - \coth(\tau - nT)]^2 - 1}. \tag{2.13}$$

From arguments in [8], we know that $\gamma > 0$.

Since equations (2.11)–(2.12) are constant coefficient linear difference equations, we assume that solutions have the form $\eta_i = A\lambda^i$ and $\mu_i = B\lambda^i$ for some constants A and B, giving

$$\begin{pmatrix} (1-\gamma)\lambda^{i-n} & \gamma\lambda^i - \lambda^{i+1} \\ \gamma\lambda^i - \lambda^{i+1} & (1-\gamma)\lambda^{i-n} \end{pmatrix} \begin{pmatrix} A \\ B \end{pmatrix} = \begin{pmatrix} 0 \\ 0 \end{pmatrix} \tag{2.14}$$

when written in matrix form. To have non-trivial solutions of equation (2.14), we need the determinant

$$(1-\gamma)^2\lambda^{2i-2n} - \gamma^2\lambda^{2i} + 2\gamma\lambda^{2i+1} - \lambda^{2i+2}$$

of the matrix in equation (2.14) to be zero. Multiplying by $-\lambda^{2n-2i}$ gives the characteristic equation

$$D_s(\lambda) := \lambda^{2n}(\lambda - \gamma)^2 - (1-\gamma)^2 = 0 \tag{2.15}$$

of the synchronous periodic solutions. The roots of $D_s(\lambda)$ are the Floquet multipliers of the synchronous periodic solution with given n, and they depend on the parameter $\gamma > 0$ from equation (2.13). Hence, the periodic solution is stable when all roots of $D_s(\lambda)$ are smaller than 1 in modulus, and a bifurcation occurs when there is a root λ with $|\lambda| = 1$. Note that $D_s(\lambda)$ in equation (2.15) factors as $D_s(\lambda) = g_s(\lambda)\tilde{g}_s(\lambda) = 0$ with

$$g_s(\lambda) = \lambda^n(\lambda - \gamma) - (1-\gamma) \tag{2.16}$$

and

$$\tilde{g}_s(\lambda) = \lambda^n(\lambda - \gamma) + (1-\gamma). \tag{2.17}$$

This is a reflection of the symmetry of equations (1.2)–(1.3): $g_s(\lambda) = 0$ is actually the characteristic equation for a single self-coupled neuron [8], which gives the stability inside the symmetry subspace with $\theta_1 = \theta_2$; and the factor $\tilde{g}_s(\lambda)$ accounts for the stability in the direction transverse to the symmetry subspace.

The properties of g_s are known from [8, Proposition 1]. For $0 < \gamma < (n+1)/n$, all roots of g_s have magnitude less than 1, and a single root leaves the unit circle with positive speed at $\lambda = 1$ as γ increases through $(n+1)/n$; this is a saddle-node bifurcation of the synchronous periodic solution. The overall stability of the synchronous periodic solution also concerns the roots of $\tilde{g}_s$, for which we have the following result.

Proposition 2.1 (Properties of the roots of $\tilde{g}_s$).

(i) For $0 < \gamma < 1$, all roots of $\tilde{g}_s$ have modulus less than 1.
(ii) At $\gamma = 1$, a root of $\tilde{g}_s$ crosses the unit circle at $\lambda = 1$ with positive speed; this is a symmetry-breaking bifurcation of the synchronous periodic solution.

Proof. (i) For any root λ of $\tilde{g}_s$, we have

$$\lambda^n(\lambda - \gamma) = -(1-\gamma) \quad \Rightarrow \quad |\lambda^n(\lambda-\gamma)| = |1-\gamma|.$$

Suppose now that $|\lambda| > 1$ and $0 < \gamma < 1$, i.e. $1 - \gamma > 0$. Then,

$$1 - \gamma = |\lambda^n(\lambda-\gamma)| \geq |\lambda|^n(|\lambda| - \gamma) > |\lambda|^n|1-\gamma| > 1-\gamma,$$

which is a contradiction.

(ii) For $\gamma = 1$, we have $\tilde{g}_s(\lambda) = \lambda^n(\lambda - 1) = 0$ and $\lambda = 1$ is a root. By differentiating equation (2.17), we obtain

$$\frac{\mathrm{d}\lambda}{\mathrm{d}\gamma} = \frac{1+\lambda^n}{\lambda^{n-1}[\lambda(n+1) - n\gamma]}.$$

Evaluating this at $\gamma = 1$, $\lambda = 1$, we obtain $\mathrm{d}\lambda/\mathrm{d}\gamma = 2 \neq 0$. This is a symmetry-breaking (or pitchfork) bifurcation due to the reflectional symmetry and because this instability concerns a direction along which θ_1 and θ_2 deviate from $\theta_1 = \theta_2$; see also §2b.

■

For the synchronous periodic solution to be stable the roots of both g_s and $\tilde{g}_s$ need to have magnitude less than 1. Since $1 < (n+1)/n$, this is the case for $0 < \gamma < 1$ (as determined by the roots of $\tilde{g}_s$). Moreover, we know from [8] that $\mathrm{d}T/\mathrm{d}\tau = 0$ when $\gamma = 1$, which means that the symmetry-breaking bifurcation, where stability is lost, takes place at the minimum on a curve in the representation in figure 1 of the branches of synchronous periodic solutions in terms of T as a function of τ; indeed, as shown, the branches are stable to the right of each minimum in T. Each branch loses another stable eigenvalue when a root of g_s passes through 1 at the saddle-node bifurcation at $\gamma = (n+1)/n$; note that, in figure 1 and its inset that this happens at the fold point of each branch with respect to τ.

The analysis above applies for $n > 0$. When $n = 0$, $g_s(\lambda) = \lambda - 1$ and $\tilde{g}_s(\lambda) = \lambda + 1 - 2\gamma$. Since $\gamma > 0$ the only instability that can occur is when $\gamma = 1$, corresponding to the symmetry-breaking bifurcation at the minimum of the black curve shown in figure 1.

(b) Bifurcating symmetry-broken synchronous periodic solutions

To find the periodic solutions that emerge from the points of symmetry breaking on the branches of synchronous periodic solutions in figure 1, we introduce a phase shift ϕ and consider

$$s_i - t_{i-n} = (n-\phi)T \quad \text{and} \quad t_i - s_{i-n} = (n+\phi)T,$$

so that $\phi = 0$ corresponds to the perfectly synchronous case. Substituting these into equations (2.7)–(2.8), we obtain the equations

$$\coth((n+1-\phi)T - \tau) = \kappa + \coth((n-\phi)T - \tau) \tag{2.18}$$

and

$$\coth((n+1+\phi)T - \tau) = \kappa + \coth((n+\phi)T - \tau), \tag{2.19}$$

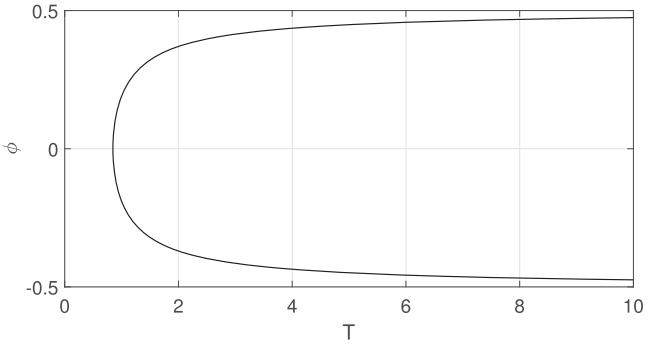

Figure 2. The relationship between the phase shift ϕ and the period T of the symmetry-broken solutions given by equation (2.21). Note the reflection symmetry about the line $\phi = 0$; thus, these solutions are created in a pitchfork bifurcation. Here, $\kappa = 5$.

for the existence of this type of periodic solution. Subtracting equation (2.18) from equation (2.19) and using $\coth x - \coth y = \sinh(x-y)/(\sinh x \sinh y)$ gives

$$\frac{\sinh(2\phi T)}{\sinh((n+1+\phi)T-\tau)\sinh((n+1-\phi)T-\tau)} = \frac{\sinh(2\phi T)}{\sinh((n+\phi)T-\tau)\sinh((n-\phi)T-\tau)}. \quad (2.20)$$

Noting that the denominators of equation (2.20) must be equal and using $\sinh x \sinh y = [\cosh(x+y) - \cosh(x-y)]/2$, we have

$$\cosh(2(n+1)T - 2\tau) = \cosh(2nT - 2\tau).$$

Since cosh is even, we conclude that one argument must be the negative of the other (since they are not equal), and it follows that the period of the symmetry-broken periodic solutions is $T = 2\tau/(2n+1)$. In turn, this means that both equations (2.18) and (2.19) reduce to

$$\coth\left(\left(\frac{1}{2} - \phi\right)T\right) = \kappa - \coth\left(\left(\frac{1}{2} + \phi\right)T\right). \quad (2.21)$$

For fixed κ, solutions of equation (2.21) lie on the curve in (T, ϕ) space that is shown in figure 2 for the specific case $\kappa = 5$. There are two branches, one for negative and one for positive ϕ, which meet at the minimum in T at $2\coth^{-1}(\kappa/2)$. In the (τ, T) plane of figure 1, the pair of solutions for given n bifurcates from the symmetry-breaking bifurcation points on the nth branch of synchronous solutions; note that both branches project to the segment of the line given by $T = 2\tau/(2n+1)$ for T above the bifurcation point. As we show in appendix A(a), all these symmetry-broken periodic solutions are unstable.

3. Alternating solutions

We now consider solutions for which the neurons take turns firing, and are half a period out of phase with one another. An example of such an alternating solution is shown in figure 3; note that, when θ reaches π from below, there is a reset of θ to $-\pi$.

To determine this type of solution, we consider the general system

$$\frac{dx}{dt} = f[x(t), y(t-\tau)] \quad (3.1)$$

and

$$\frac{dy}{dt} = f[y(t), x(t-\tau)], \quad (3.2)$$

and suppose that it has an alternating periodic solution with period T, which means $y(t) = x(t + T/2)$ and, hence, $y(t-\tau) = x(t - \tau + T/2) = x(t - (\tau - T/2))$. Thus, this solution is also a periodic

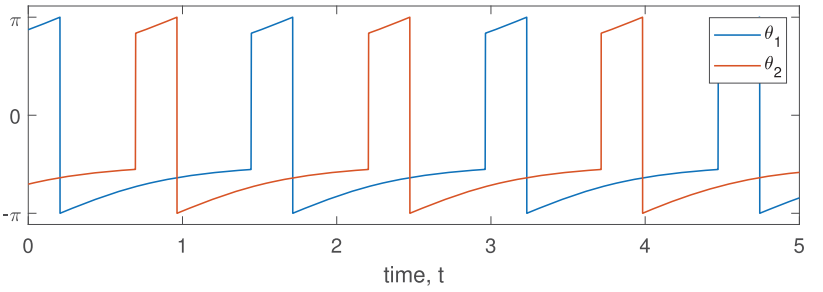

Figure 3. Alternating periodic solution of equations (1.2)–(1.3) for $\kappa = 5$ and $\tau = 2$. Note that, when θ_i reaches π from below, it is reset to $-\pi$.

solution of period T of the *self-coupled* system

$$\frac{dx}{dt} = f[x(t), x(t-(\tau - T/2))]$$

with a delay of $\tau - T/2$. Similarly, if we find a periodic solution with period T of the system

$$\frac{dx}{dt} = f(x(t), x(t-\tau)) \tag{3.3}$$

(as we did in [8]), then this solution is also a periodic solution of period T of the system

$$\frac{dx}{dt} = f[x(t), y(t-(\tau + T/2))]$$

and

$$\frac{dy}{dt} = f[y(t), x(t-(\tau + T/2))],$$

for which x and y alternate.

Therefore, since periodic solutions of a single delay-coupled theta neuron of the form equation (3.3) are given by equation (2.4), the existence of alternating solutions of equations (1.2)–(1.3) is given by equation (2.4) when replacing τ by $\tau - T/2$; i.e. the existence of alternating solution is given by the equation

$$\coth[(n+1/2)T - \tau] = \kappa + \coth[(n-1/2)T - \tau], \tag{3.4}$$

for $\kappa > 2$, which is valid for $(n-1/2)T < \tau < (n+1/2)T$. Note that equation (3.4) can also be obtained from equation (2.4) by replacing n by $n - 1/2$; however, the physical meaning of this replacement is not clear since n is an integer. The meaning of n in equation (3.4) is that if neuron 1 fires at time 0, there are n past firing times of neuron 2 in the interval $(-\tau, 0)$; note that n could be zero.

(a) Stability of alternating solutions

To determine the stability of alternating solutions, we need to consider two cases that depend on the value of the delay τ relative to the value of the multiple nT of the basic period T. While the derivation differs, the resulting equation is actually the same for the two cases. To provide insight into the idea behind either derivation, we show in figure 4 a schematic of case 1 described below in §3a(i), specifically, for $\tau = 4$, $T = 6$ and $n = 1$.

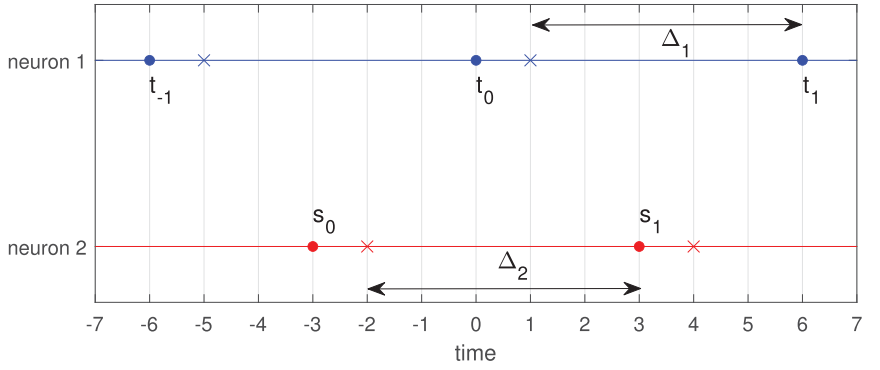

Figure 4. Schematic of firing times (circles) and times at which the neuron's phase is instantaneously increased (crosses). Here, the delay is $\tau = 4$, the period is $T = 6$ and $n = 1$; the times $\Delta_{1,2}$ are defined in §3a(i).

(i) Case 1 where $(n - 1/2)T < \tau < nT$

In figure 4 with $n = 1$, neuron 1 has just fired at time $t = 0$. After time $\tau - (t_0 - s_{1-n})$, its angle θ_1 equals

$$\theta_1^- = 2\tan^{-1}\left[-\coth\left(\tau - (t_0 - s_{1-n})\right)\right] \tag{3.5}$$

and this is reset to θ_1^+, where

$$\tan\left(\theta_1^+/2\right) = \tan\left(\theta_1^-/2\right) + \kappa.$$

This event is marked with the blue cross at $t = 1$ in figure 4. There is then a wait time Δ_1 before neuron 1 fires, which from equation (2.3) is

$$\Delta_1 = \coth^{-1}\left[\tan\left(\frac{\theta_1^+}{2}\right)\right]. \tag{3.6}$$

Hence, $t_1 = t_0 + \tau - (t_0 - s_{1-n}) + \Delta_1 = \tau + s_{1-n} + \coth^{-1}\left[\kappa - \coth\left(\tau - (t_0 - s_{1-n})\right)\right]$.

Going back to when neuron 2 last fired at s_0, in complete analogy, after time $\tau - (s_0 - t_{-n})$, we have

$$\theta_2^- = 2\tan^{-1}\left[-\coth\left(\tau - (s_0 - t_{-n})\right)\right] \tag{3.7}$$

and θ_2 is reset to θ_2^+, where

$$\tan\left(\theta_2^+/2\right) = \tan\left(\theta_2^-/2\right) + \kappa.$$

This reset is marked with the red cross at $t = -2$ in figure 4. The corresponding wait time Δ_2 before neuron 2 fires is

$$\Delta_2 = \coth^{-1}\left[\tan\left(\frac{\theta_2^+}{2}\right)\right], \tag{3.8}$$

giving $s_1 = s_0 + \tau - (s_0 - t_{-n}) + \Delta_2 = \tau + t_{-n} + \coth^{-1}\left[\kappa - \coth\left(\tau - (s_0 - t_{-n})\right)\right]$.

We calculated s_1 and t_1 in terms of previous firing times, but the calculation is entirely general, and we conclude for any $i = 0, 1, 2, \ldots$ that

$$s_{i+1} = \tau + t_{i-n} + \coth^{-1}\left[\kappa - \coth\left(\tau - s_i + t_{i-n}\right)\right] \tag{3.9}$$

and

$$t_{i+1} = \tau + s_{i+1-n} + \coth^{-1}\left[\kappa - \coth\left(\tau - t_i + s_{i+1-n}\right)\right]. \tag{3.10}$$

(ii) Case 2 where $nT < \tau < (n + 1/2)T$

For this range of τ, suppose that neuron 1 has just fired at $t = t_0 = 0$ and the previous firing of neuron 2 was at $s_0 < t_0$. Then, $\theta_2(0) = 2\tan^{-1}[-\coth(t_0 - s_0)]$ and, after a time $\tau - (t_0 - t_{-n})$, the angle θ_2 equals

$$\begin{aligned}\theta_2^- &= 2\tan^{-1}\left[-\coth\left(\tau - (t_0 - t_{-n}) - \coth^{-1}\left[\tan\left(\frac{\theta_2(0)}{2}\right)\right]\right)\right] \\ &= 2\tan^{-1}[-\coth(\tau - (s_0 - t_{-n}))].\end{aligned}$$

This is exactly equation (3.7) and gives the same reset to θ_2^+. Therefore, the wait time Δ_2 before neuron 2 fires is also given by equation (3.8), which yields

$$s_1 = t_0 + \tau - (t_0 - t_{-n}) + \Delta_2 = \tau + t_{-n} + \coth^{-1}[\kappa - \coth^{-1}(\tau - (s_0 - t_{-n}))]. \tag{3.11}$$

To find t_1, we know that neuron 1 has just fired at t_0. In complete analogy, after time $\tau - (t_0 - s_{1-n})$, we have $\theta_1 = \theta_1^-$ as given by equation (3.7), with the same reset to θ_1^+ and subsequent wait time Δ_1 given by equation (3.6), yielding

$$t_1 = t_0 + \tau - (t_0 - s_{1-n}) + \Delta_1 = \tau + s_{1-n} + \coth^{-1}[\kappa - \coth(\tau - (t_0 - s_{1-n}))]. \tag{3.12}$$

As for case 1, these calculations are again entirely general and, in fact, equations (3.11) and (3.12) also give equations (3.9)–(3.10) for any for $i = 0, 1, 2, \ldots$. Note that equation (3.9) is the same expression for s_{i+1} that we found §2a for the existence of synchronous solutions; the difference for alternating solutions lies in expression equation (3.10) for t_{i+1}.

(iii) Linearization around the alternating solution

To linearize around a periodic solution given by equations (3.9)–(3.10), we write these equations as

$$R(s_{i+1}, t_{i-n}, s_i) = 0$$

and

$$S(t_{i+1}, s_{i-n+1}, t_i) = 0.$$

As in §2a, we perturb the firing times as $s_i \to s_i + \mu_i$ and $t_i \to t_i + \eta_i$ and obtain to first order

$$\frac{\partial R}{\partial s_{i+1}}\mu_{i+1} + \frac{\partial R}{\partial t_{i-n}}\eta_{i-n} + \frac{\partial R}{\partial s_i}\mu_i = 0$$

and

$$\frac{\partial S}{\partial t_{i+1}}\eta_{i+1} + \frac{\partial S}{\partial s_{i-n+1}}\mu_{i-n+1} + \frac{\partial S}{\partial t_i}\eta_i = 0,$$

which, after calculating the partial derivatives, we write as

$$-\mu_{i+1} + (1 - \gamma_1)\eta_{i-n} + \gamma_1\mu_i = 0 \tag{3.13}$$

and

$$-\eta_{i+1} + (1 - \gamma_2)\mu_{i-n+1} + \gamma_2\eta_i = 0, \tag{3.14}$$

where

$$\gamma_1 = \frac{1 - \coth^2(\tau + t_{i-n} - s_i)}{1 - [\kappa - \coth(\tau + t_{i-n} - s_i)]^2} \tag{3.15}$$

and

$$\gamma_2 = \frac{1 - \coth^2(\tau - t_i + s_{i-n+1})}{1 - [\kappa - \coth(\tau - t_i + s_{i-n+1})]^2}. \tag{3.16}$$

For an alternating periodic solution, we have

$$\gamma := \gamma_1 = \gamma_2 = \frac{\coth^2(\tau - (n - 1/2)T) - 1}{[\kappa - \coth(\tau - (n - 1/2)T)]^2 - 1}. \tag{3.17}$$

Note that, when replacing n by $n+1/2$ in this expression for γ, we obtain exactly equation (2.13); in particular, again $\gamma > 0$.

As before for equations (2.11)–(2.12), we consider solutions $\eta_i = A\lambda^i$ and $\mu_i = B\lambda^i$ with $A, B \in \mathbb{R}$ and write the linear difference equations (3.13)–(3.14) with γ as in equation (3.17) as the matrix equation

$$\begin{pmatrix} (1-\gamma)\lambda^{i-n} & \gamma\lambda^i - \lambda^{i+1} \\ \gamma\lambda^i - \lambda^{i+1} & (1-\gamma)\lambda^{i-n+1} \end{pmatrix} \begin{pmatrix} A \\ B \end{pmatrix} = \begin{pmatrix} 0 \\ 0 \end{pmatrix}.$$

Its determinant is

$$(1-\gamma)^2\lambda^{2i-2n+1} - \gamma^2\lambda^{2i} + 2\gamma\lambda^{2i+1} - \lambda^{2i+2} \tag{3.18}$$

for given integer n.

The case $n = 0$ is special and gives, by setting equation (3.18) to zero and then multiplying by $-\lambda^{-2i}$, the characteristic equation

$$\lambda^2 - (1+\gamma^2)\lambda + \gamma^2 = (\lambda - 1)(\lambda - \gamma^2) = 0 \tag{3.19}$$

of the alternating periodic solutions with $n = 0$. We see that $\lambda = 1$ is always a solution; it is the trivial Floquet multiplier representing the invariance of periodic solutions under time translation. From the other factor of equation (3.19), we conclude that the alternating periodic solution with $n = 0$ is stable for $0 < \gamma < 1$ and unstable for $1 < \gamma$.

For $n \geq 1$ in equation (3.18), we obtain with multiplication by $-\lambda^{2n-1-2i}$ the characteristic equation

$$D_a(\lambda) := \lambda^{2n-1}(\lambda - \gamma)^2 - (1-\gamma)^2 = 0 \tag{3.20}$$

of the alternating periodic solutions with $n \geq 1$. We remark that $D_s(\lambda)$ from equation (2.15) is obtained from $D_a(\lambda)$ by the substitution $n \mapsto n + 1/2$. In particular, this characteristic equation also factors, as $D_a(\lambda) = g_a(\lambda)\tilde{g}_a(\lambda) = 0$ but now with

$$g_a(\lambda) = \lambda^{n-1/2}(\lambda - \gamma) - (1-\gamma)$$

and

$$\tilde{g}_a(\lambda) = \lambda^{n-1/2}(\lambda - \gamma) + (1-\gamma).$$

These two polynomials in $\rho = \sqrt{\lambda}$, which determine the stability inside the symmetry subspace of the alternating solutions and in the direction transverse to it, respectively, can be treated individually. However, we find it more convenient to consider $D_a(\lambda)$ in equation (2.15) 'holistically' and to factor it via its trivial root $\lambda = 1$ as $D_a(\lambda) = (\lambda - 1)H_a(\lambda)$, where

$$H_a(\lambda) = \lambda^{2n} + (1-2\gamma)\lambda^{2n-1} + (1-\gamma)^2 \sum_{i=0}^{2n-2} \lambda^i.$$

We have the following statements for the stability of the alternating periodic solutions with $n \geq 1$.

Proposition 3.1 (Properties of the roots of D_a and H_a).

(i) When $\gamma = 0$, the roots of D_a are the $(2n+1)$th roots of unity; in particular, they all have modulus 1.
(ii) When $\gamma = 1$, the polyonomial H_a has the single root 1, as well as the root 0 with multiplicity $2n-1$ when $n \geq 1$.
(iii) If $H_a(1) = 0$ then either $\gamma = 1$ or $\gamma = (2n+1)/(2n-1)$.
(iv) If $0 < \gamma < 1$, then no roots of D_a are outside the unit circle, i.e. the alternating periodic solution is not unstable.
(v) At both $\gamma = 1$ and $\gamma = (2n+1)/(2n-1)$, a real root of D_a transversely leaves the unit circle as γ increases.
(vi) $\gamma = 1$ is at the minimum of the graph of T as a function of τ; at this point, there is the switch from case 1 to case 2 in the derivation of our stability results.
(vii) At $\gamma = (2n+1)/(2n-1)$, there is a saddle-node bifurcation of alternating periodic solutions.

royalsocietypublishing.org/journal/rspa Proc. R. Soc. A 481: 20240897

(viii) At $\gamma = 1$, there is a symmetry bifurcation of alternating periodic solutions.

Proof.

(i) If $\gamma = 0$ then $D_a(\lambda) = \lambda^{2n+1} - 1 = 0$ and the result follows. (Note that while γ can tend to 0, it never actually reaches that value.)
(ii) If $\gamma = 1$ then $H_a(\lambda) = \lambda^{2n} - \lambda^{2n-1} = \lambda^{2n-1}(\lambda - 1) = 0$ and the result follows.
(iii) If $H_a(1) = 0$ then $1 + (1 - 2\gamma) + (1 - \gamma)^2(2n - 1) = 0$, and solving this quadratic equation for γ gives the result.
(iv) Suppose $D_a(\lambda) = 0$, i.e.

$$\lambda^{2n-1}(\lambda - \gamma)^2 = (1 - \gamma)^2 \Rightarrow |\lambda^{2n-1}(\lambda - \gamma)^2| = (1 - \gamma)^2. \tag{3.21}$$

Assume now that $|\lambda| > 1$. Then $|\lambda^{2n-1}(\lambda - \gamma)^2| > (1 - \gamma)^2$, which contradicts equation (3.21); thus, we cannot have $|\lambda| > 1$.
(v) Differentiating $D_a(\lambda) = 0$ with respect to γ, we get

$$\frac{\mathrm{d}\lambda}{\mathrm{d}\gamma} = \frac{2[(\lambda - \gamma)\lambda^{2n-1} + \gamma - 1]}{\lambda^{2n-2}[(2n-1)\gamma^2 - 4n\gamma\lambda + (2n+1)\lambda^2]}.$$

If $\lambda = 1$ and $(2n-1)\gamma^2 - 4n\gamma + 2n + 1 \neq 0$ (i.e. $\gamma \neq 1$ and $\gamma \neq (2n+1)/(2n-1)$; compare with (iii)) then $\mathrm{d}\lambda/\mathrm{d}\gamma = 1$, reflecting that the root $\lambda = 1$ of D_a is always present. However, if $\gamma = 1$ then

$$\frac{\mathrm{d}\lambda}{\mathrm{d}\gamma} = \frac{2\lambda(\lambda - 1)}{2n - 1 - 4n\lambda + (2n+1)\lambda^2},$$

which is undefined at $\lambda = 1$. With l'Hopital's rule, we conclude that

$$\lim_{\lambda \to 1} \frac{\mathrm{d}\lambda}{\mathrm{d}\gamma} = \lim_{\lambda \to 1} \frac{4\lambda - 2}{2\lambda(2n+1) - 4n} = 1 > 0.$$

Similarly if $\gamma = (2n+1)/(2n-1)$ then

$$\frac{\mathrm{d}\lambda}{\mathrm{d}\gamma} = \frac{2[\lambda(2n-1) - (2n+1)]\lambda^{2n-1} + 4}{\lambda^{2n-2}[(2n+1)^2 - 4n(2n+1)\lambda + (4n^2-1)\lambda^2]},$$

which is also undefined at $\lambda = 1$. Again, with l'Hopital's rule, we have

$$\lim_{\lambda \to 1} \frac{\mathrm{d}\lambda}{\mathrm{d}\gamma} = \lim_{\lambda \to 1} \frac{\lambda(2n-1)(2n\lambda - 2n - 1)}{4n^3(\lambda - 1)^2 - n[(\lambda - 2)\lambda + 3] - 1} = \frac{2n-1}{2n+1} > 0,$$

where we used that $n \geq 1$.
(vi) Since equation (3.4) defines T as a function of τ, we can differentiate it with respect to τ to get

$$\operatorname{csch}^2[(n+1/2)T - \tau]\left[(n+1/2)\frac{\mathrm{d}T}{\mathrm{d}\tau} - 1\right] = \operatorname{csch}^2[(n-1/2)T - \tau]\left[(n-1/2)\frac{\mathrm{d}T}{\mathrm{d}\tau} - 1\right]. \tag{3.22}$$

Setting $\mathrm{d}T/\mathrm{d}\tau = 0$, we get (by taking reciprocals)

$$\coth^2[(n+1/2)T - \tau] = \coth^2[(n-1/2)T - \tau].$$

We cannot have

$$\coth[(n+1/2)T - \tau] = \coth[(n-1/2)T - \tau]$$

because that would imply from equation (3.4) that $\kappa = 0$, which is not possible, so we conclude that

$$\coth[(n+1/2)T - \tau] = -\coth[(n-1/2)T - \tau]. \tag{3.23}$$

Substituting equations (3.23) into (3.4), we obtain

$$\kappa = -2\coth[(n-1/2)T - \tau] = 2\coth[\tau - (n-1/2)T],$$

and substituting this into equation (3.17) we find $\gamma = 1$, as required. From equation (3.23), we have $(n + 1/2)T - \tau = \tau - (n - 1/2)T$ which can be rearranged to the condition $\tau = nT$ for switching between cases 1 and 2.

(vii) We first write γ from equation (3.17) as

$$\begin{aligned}\gamma &= \frac{\coth^2[(n-1/2)T-\tau]-1}{\{\kappa+\coth[(n-1/2)T-\tau]\}^2-1}\\ &= \frac{\coth^2[(n-1/2)T-\tau]-1}{\coth^2[(n+1/2)T-\tau]-1}\\ &= \frac{\operatorname{csch}^2[(n-1/2)T-\tau]}{\operatorname{csch}^2[(n+1/2)T-\tau]},\end{aligned} \tag{3.24}$$

where we used equation (3.4) to get the second line. We also rearrange equation (3.22) to obtain

$$\frac{\mathrm{d}T}{\mathrm{d}\tau} = \frac{\operatorname{csch}^2[(n+1/2)T-\tau]-\operatorname{csch}^2[(n-1/2)T-\tau]}{\operatorname{csch}^2[(n+1/2)T-\tau](n+1/2)-\operatorname{csch}^2[(n-1/2)T-\tau](n-1/2)}. \tag{3.25}$$

Now, if $\gamma = (2n+1)/(2n-1)$ then, from equation (3.24),

$$(2n-1)\operatorname{csch}^2[(n-1/2)T-\tau] = (2n+1)\operatorname{csch}^2[(n+1/2)T-\tau],$$

and, thus, the denominator of equation (3.25) is zero. However, the numerator of equation (3.25) is not zero (since $\gamma \neq 1$); hence, the graph of T as a function of τ has an infinite slope. This identifies the change of stability at $\gamma = (2n+1)/(2n-1)$ from (v) as a saddle-node bifurcation.

(viii) Since we have a minimum of T as a function of τ at $\gamma = 1$, with derivative zero, the change of stability according to (v) at this point is not a saddle-node bifurcation. In light of the symmetry of equations (1.2)–(1.3), this is indeed a symmetry-breaking (pitchfork) bifurcation.

■

(b) Branches of alternating periodic solutions

The branches of alternating solutions given by equation (3.4) are shown in figure 5 for $\kappa = 5$ and n up to 4, with stability information as given by proposition 3.1. The branch for $n = 0$ plays a special role, and we describe it first. This branch of alternating solutions is symmetric with respect to reflection about the T-axis, and it has the minimum $\overline{T} = 2\coth^{-1}(\kappa/2)$ at $\tau = 0$. Moreover, $0 < \gamma < 1$ for $\tau > 0$ and $1 < \gamma$ for $\tau < 0$. This means that the alternating solutions with $n = 0$ and $\tau > 0$ are stable; however, those with $\tau < 0$ are not. From the minimum, where $\gamma = 1$, a vertical branch of symmetry-broken alternating solutions for $\tau = 0$ emerges; they are discussed below in §3c. The stable branch for $n = 0$ is interesting since it persists down to $\tau = 0$, i.e. such an alternating solution exists even without delays. This can be understood as follows. Suppose neuron 1 fires. This immediately pushes neuron 2 past its threshold but, since it takes a finite time for neuron 2 to then fire, the influence of neuron 2 firing is not immediately felt by neuron 1. Due to this reaction time, neuron 2 effectively provides delayed feedback of neuron 1 to itself (and vice versa, by swapping neuron labels).

All branches with $n \geq 1$ also have the minimum $\overline{T} = 2\coth^{-1}(\kappa/2)$, where the stability changes, as well as a point of saddle-node bifurcation. As stated in proposition 3.1, γ varies monotonically along each of these branches, and it is between 0 and 1 to the right of the minimum; hence, these alternating solutions, which are described by case 1, are stable. Each minimum is a symmetry-breaking bifurcation, and a branch of symmetry-broken alternating solutions emerges. These branches are already shown in figure 5, and they are discussed in §3c. The alternating solutions to the other side of the minimum along any branch with $n \geq 1$ are described by case 2 and unstable.

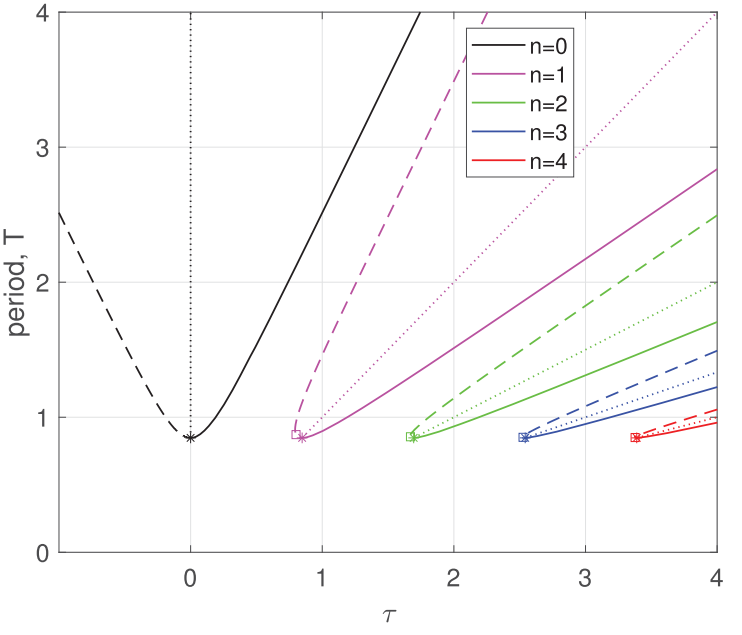

Figure 5. Branches of alternating periodic solutions of equations (1.2)–(1.3) with $n = 0, 1, 2, 3, 4$. Solid curves are stable (to the right of each minimum) and dashed curves are unstable. Saddle-node bifurcations are marked with squares, symmetry-breaking bifurcations with stars and bifurcating pairs of symmetry-broken solutions are represented by dotted lines. Here, $\kappa = 5$.

Continuing along a branch, a second multiplier leaves the unit circle through 1 at the saddle-node bifurcation where $\gamma = (2n + 1)/(2n - 1)$. Along the respective upper branch, the alternating periodic solutions have two unstable directions.

(c) Bifurcating symmetry-broken alternating periodic solutions

We first consider the symmetry-broken alternating periodic solutions for the special case that $n = 0$, which bifurcate from the minimum at $\tau = 0$ and exist along the vertical dashed line in figure 5. Since there is no delay, equations (1.2)–(1.3) can be visualized in the phase space $\mathbb{S}^1 \times \mathbb{S}^1$ of the periodic variables θ_1 and θ_2, which we represent by the square $[0, 2\pi] \times [0, 2\pi]$ subject to identification of its left and right, and lower and upper boundaries. The firing with reset of the two neurons occurs along the lines where $\theta_1 = \pi$ and $\theta_2 = \pi$. Between firings, the flow is given by the system of the two ordinary differential equations (ODEs)

$$\frac{d\theta_1}{dt} = -2\cos\theta_1 \tag{3.26}$$

and

$$\frac{d\theta_2}{dt} = -2\cos\theta_2, \tag{3.27}$$

which has four equilibria: the source $(\pi/2, \pi/2)$, the sink $(3\pi/2, 3\pi/2)$, and the saddles $(\pi/2, 3\pi/2)$ and $(3\pi/2, \pi/2)$. As is shown in figure 6, these equilibria are connected by the stable and unstable invariant manifolds of the saddles, which are vertical and horizontal lines because equations (3.26) and (3.27) are decoupled. Note the symmetry of figure 6 with respect to reflection in the diagonal, due to the exchange symmetry $(\theta_1, \theta_2) \mapsto (\theta_2, \theta_1)$.

To find periodic solutions of equations (3.26)–(3.27), we assume that θ_2 has just fired, i.e. $\theta_2 = \pi$ and $\theta_1 = \alpha$. As is clear from figure 6, when $0 \le \alpha < \pi/2$ or $3\pi/2 \le \alpha \le 2\pi$ the trajectory will approach the attractor $(\theta_1, \theta_2) = (3\pi/2, 3\pi/2)$. For $\alpha = \pi/2$, the trajectory approaches the saddle equilibrium $(\theta_1, \theta_2) = (\pi/2, 3\pi/2)$ since this initial point lies on its stable manifold. However,

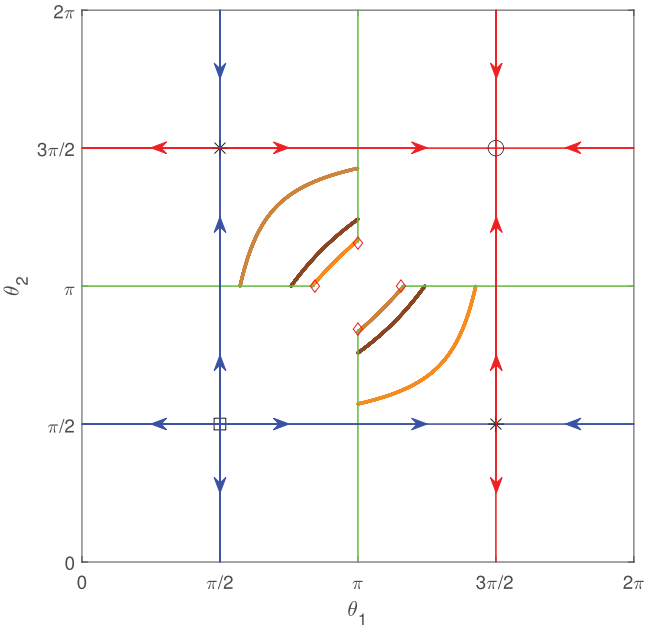

Figure 6. Illustration of alternating periodic solutions of equation (1.2)–(1.3) with $\tau = 0$ as trajectories of equation (3.26)–(3.27) on the square $[0, 2\pi] \times [0, 2\pi]$ with the firing lines (green) where one phase increases through π and a discontinuous reset occurs. Shown is a pair of symmetry-broken periodic solutions (light brown and orange curves), which pass through $(\theta_1, \theta_2) = (1.6, \pi)$ and $(\theta_1, \theta_2) = (2\pi - 1.6, \pi)$, respectively, and the symmetric periodic solution at the point of symmetry breaking (brown curves), which has the minimum period $\overline{T} = 2\coth^{-1}(\kappa/2)$ and passes through $(\theta_1, \theta_2) = (2\tan^{-1}(\kappa/2), \pi)$ and $(\theta_1, \theta_2) = (2\pi - 2\tan^{-1}(\kappa/2), \pi)$. Also shown are the repellor (square), the attractor (circle), the two saddle equilibria (crosses) and their stable and unstable manifolds (blue and red horizontal and vertical lines). The red diamonds bound the ranges of θ_1 and θ_2 along which any alternating periodic solutions with $\tau = 0$ must fire. Here, $\kappa = 5$.

when $\pi/2 < \alpha < \pi$ both θ_1 and θ_2 increase until the firing line with $\theta_1 = \pi$ is reached at $\theta_2 = 2\tan^{-1}[-\coth(\Delta_1)] = 2\pi - \alpha$ after the time $\Delta_1 = \coth^{-1}[\tan(\alpha/2)]$. At this point, θ_2 is reset and incremented to $\theta_2^+ = 2\tan^{-1}(\kappa + \tan(\pi - \alpha/2))$, which we assume is greater than $\pi/2$ (otherwise the system approaches an equilibrium). Both phases then continue to increase until $\theta_2 = \pi$, which takes a further time $\Delta_2 = \coth^{-1}[\tan(\theta_2^+/2)]$, at which point $\theta_1 = 2\tan^{-1}[-\coth(\Delta_2)] = 2\pi - \theta_2^+$. Now θ_1 is reset and incremented to $\theta_1^+ = 2\tan^{-1}(\kappa + \tan(\pi - \theta_2^+/2))$. For this process to yield a periodic solution, we need $\theta_1^+ = \alpha$, which is, in fact, true for any α that results in a return to this firing line. This is due to the special form of equations (3.26)–(3.27) and the symmetry of cos around π: the angle θ_1 increases from α to π by the same amount as θ_2, which therefore increases to $2\pi - \alpha$; the equivalent statement is true for the second 'leg' of the periodic solution with $\theta_1 > \pi$.

Hence, there is a one-parameter family of (pairs of) symmetry-broken periodic solutions. The pair for $\alpha = 1.6$ and $\alpha = 2\pi - 1.6$ is shown in figure 6; also shown is the symmetric alternating periodic solution for $\alpha = 2\tan^{-1}(\kappa/2)$ with period $\overline{T} = 2\coth^{-1}(\kappa/2)$, from which the family of symmetry-broken periodic solutions bifurcate. More generally, the existence of this family of periodic solutions is due to the fact that system equations (3.26)–(3.27) is reversible; specifically, it is invariant under the transformation $(t, \theta_1, \theta_2) \mapsto (-t, -\theta_1, -\theta_2)$, which is the rotation by π about the origin (and any π translates) with time reversal. In light of the exchange symmetry, the reversibility manifests itself in figure 6 as the reflection in the antidiagonal, subject to the reversal of time t.

The condition that $\pi/2 < \theta_2^+$ to obtain a periodic solution is equivalent to $\tan(\alpha/2) < \kappa - 1$ and, thus, restricts the valid range for α to the intervals $(\pi/2, \alpha^*)$ and $(\pi/2, 2\pi - \alpha^*)$ with $\alpha^* =$

$2\tan^{-1}(\kappa-1)$. The corresponding points (α^*,π) and $(2\pi-\alpha^*,\pi)$ on the θ_2-firing line, as well as (π,α^*) and $(\pi,2\pi-\alpha^*)$ on the θ_1-firing line, represent the 'inner' limit of the family of symmetry-broken alternating solutions; these four points are marked in figure 6. The other limit of this family for $\alpha\searrow\pi/2$ and for $\alpha\nearrow 3\pi/2$ is formed by the respective parts of the invariant manifolds of the two saddles. Note that $\alpha^*\to\pi/2$ as $\kappa\searrow 2$, and for $\kappa\leq 2$ alternating solutions with $\tau=0$ do not exist.

The period of any solution of the family is $T=\Delta_1+\Delta_2$, and we can write $\Delta_1=(1/2+\phi)T$ and $\Delta_2=(1/2-\phi)T$ for some $-1/2<\phi<1/2$. We find that $\coth(\Delta_1)=\tan(\alpha/2)$ and $\coth(\Delta_2)=\kappa-\tan(\alpha/2)$ and, thus, $\coth(\Delta_2)=\kappa-\coth(\Delta_1)$, or

$$\coth((1/2-\phi)T)=\kappa-\coth((1/2+\phi)T), \tag{3.28}$$

which is exactly equation (2.21). Hence, the graph of the period of the symmetry-broken alternating solutions as a function of ϕ is that shown in figure 2, for which the minimum period $\overline{T}=2\coth^{-1}(\kappa/2)$ occurs when $\Delta_1=\Delta_2$, i.e. when $\alpha=2\tan^{-1}(\kappa/2)$. As we show in appendix A(b), the periodic solutions with $\tau=0$ are neutrally stable, which is consistent with there being a continuum of them.

To find the branches of symmetry-broken alternating periodic solutions for $n\geq 1$ with $\tau>0$, we use the concept of reappearance [27]: a periodic solution with $\tau=0$ with a given ϕ and T satisfying equation (3.28) is also a periodic solution with the same ϕ and T when the delay equals an integer multiple nT of the period T. These symmetry-broken solutions, hence, lie on the straight line segments $T=\tau/n$ with $T>2\coth^{-1}(\kappa/2)$, which emerge from the minima, the points of symmetry-breaking bifurcations, on the branch of alternating periodic solutions for the respective $n\geq 1$. All these symmetry-broken solutions are unstable, as we show in appendix A(c).

(d) Overall picture of periodic solutions

We finish our investigation by presenting together in figure 7 the branches of synchronous and alternating periodic solutions and the respective branches of symmetry-broken solutions; here, (a) shows the combined solution branches for $\kappa=5$ from figures 1 and 5, and (b) shows the equivalent image for $\kappa=3$. Figure 7 shows that the two types of periodic solution branches interleave, with symmetry-broken solutions of one type fitting into the 'gaps' between branches of the other type. Note that the 'neighbouring' curves forming these gaps have the limiting slopes $T=\tau/n$ of the respective line segment of symmetry-broken solutions. As we observed earlier, the consecutive branches (with larger and larger τ-values of their minima) map to one another when the transformation $n\mapsto n+1/2$ is applied to their respective parametrization, which entails a switch of type; note that this mapping is consistent with the stability properties: the branches of synchronized and of alternating periodic solutions are qualitatively the same in this regard.

We concentrated on investigating the effects of varying the delay τ, but it is also of interest to vary the coupling strength κ. For all of the periodic solutions we found, κ must be greater than 2. This is the result of setting $I=-1$ at the start of the paper, as the Dirac delta function coupling must be strong enough to kick a neuron across the 'gap' between the stable and unstable equilibria of the theta neuron (whose position is related to I) to trigger its firing. As κ is decreased towards $\kappa=2$, the distance between the branches increases, but note that the slopes of the branches of symmetry-broken solutions are independent of κ. In the limit $\kappa\searrow 2$, all branches with minima disappear to the right, towards infinitely large values of τ, and the stable branch of alternating solutions with $n=0$ is the only one left in the region with $\tau>0$.

When κ is increased, on the other hand, all symmetry-breaking and saddle-node bifurcation points approach the origin of the (τ,T)-plane. Specifically, the minimum period $T=2\coth^{-1}(\kappa/2)$ of solution branches in figure 7 goes to zero, and the gaps between the stable part of the nth and the unstable part of the $(n+1)$th branch of the same type shrink to zero as well. The

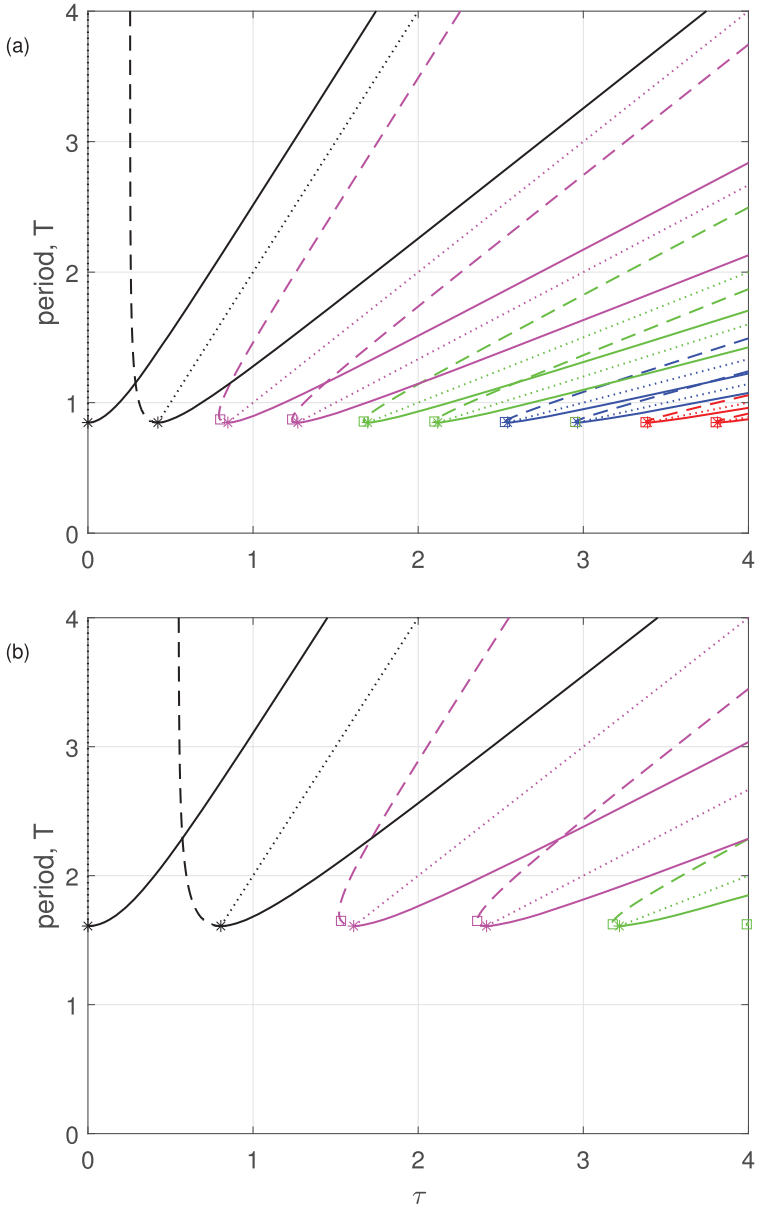

Figure 7. All solution branches found in §§2 and 3 plotted together, for $\kappa = 5$ in (a) and for $\kappa = 3$ in (b). Symbols and colours for each n are as in figures 1 and 5; the leftmost curve of the same colour is that of alternating solutions and the rightmost one of synchronous solutions. Note the increasing degree of multistability with τ, including between the two types of solutions.

dynamics are considerably simplified in the limit $\kappa \to \infty$. From equation (1.4), we see that, in this case, the influence of a past firing of a neuron is to cause the receiving neuron to immediately fire. From equation (2.4), synchronous periodic solution therefore exist for $T = \tau/(n+1)$. From equation (2.13), we have $\gamma = 0$ and, thus, from equation (2.15), these solutions are neutrally stable. Similar arguments show that alternating periodic solutions exist for $T = \tau/(n+1/2)$ and are also neutrally stable. Moreover, no symmetry-broken solutions exist. Hence, the limit $\kappa \to \infty$ in the (τ, T)-plane is an infinite fan of interleaving rays from the origin, of synchronous and alternating periodic solutions, with the rays accumulating on the τ-axis.

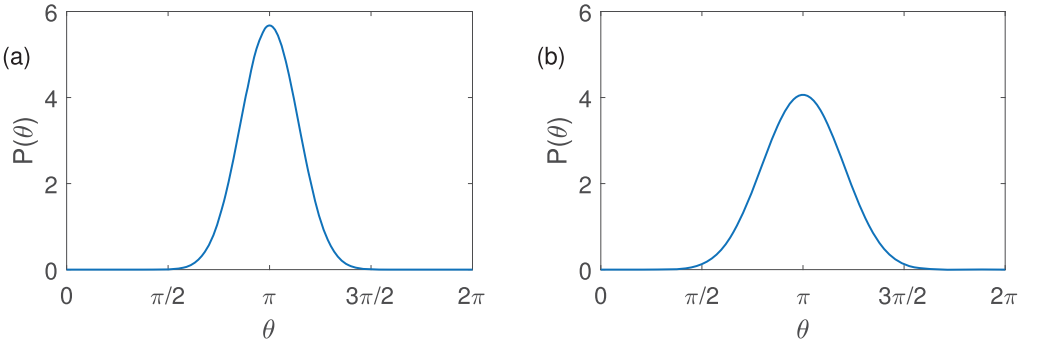

Figure 8. The pulsatile function $P(\theta)$ for $m = 10$ in (a) and $m = 5$ in (b).

4. Two theta neurons coupled with smooth feedback

We now consider the case of smooth feedback with the pulsatile function centred at $\theta = \pi$ given by

$$P(\theta) = a_m(1 - \cos\theta)^m, \tag{4.1}$$

where $a_m = 2^m(m!)^2/(2m)!$ ensures that $\int_0^{2\pi} P(\theta)d\theta = 2\pi$ for all m; see also [8]. Increasing m makes this function 'sharper', and in the limit $m \to \infty$, we have $P(\theta) = 2\pi\delta(\theta - \pi)$, where δ is the Dirac delta function. With this smooth feedback, the equations of the two coupled theta neurons are

$$\frac{d\theta_1}{dt} = 1 - \cos\theta_1 + (1 + \cos\theta_1)(-1 + \kappa P[\theta_2(t - \tau)]) \tag{4.2}$$

and

$$\frac{d\theta_2}{dt} = 1 - \cos\theta_2 + (1 + \cos\theta_2)(-1 + \kappa P[\theta_1(t - \tau)]), \tag{4.3}$$

which is a DDE with the constant delay τ that has equations (1.2)–(1.3) as its limit for $m \to \infty$ (although with a different value of κ).

We proceed by discussing the branches of its different types of periodic solutions, as well as their stability properties; this information is no longer available analytically, but it can be found with the continuation package DDE-BIFTOOL [28]. Specifically, we consider $P(\theta)$ for the two cases $m = 10$ and $m = 5$ that are shown in figure 8.

(a) Synchronized solutions

Figure 9 shows the branches of synchronized periodic solutions of equations (4.2)–(4.3) with $\kappa = 5$ and for $m = 10$ in (a) and $m = 3$ in (b). They were obtained by continuing the respective stable periodic solution in the delay τ, while monitoring the Floquet multipliers to detect bifurcations due to stability changes. The symmetry-broken synchronized periodic solutions were continued from the symmetry-breaking points by making use of the branch switching capability of DDE-BIFTOOL. The branches of the different periodic solutions are very close to and qualitatively the same as those in figure 1a. In particular, as for the limiting case of a Dirac delta function coupling, the branches in figure 9 emerge for increasing τ at saddle-node bifurcations and there is a symmetry-breaking (pitchfork) bifurcation at the minimum of each branch, with a stable part of the branch to its right. Note that the branches of symmetry-broken periodic solutions still lie exactly on the lines $T = 2\tau/(2n + 1)$, indicating that this is a property of the solutions rather than the specific form of the model.

These statements are true for both $m = 10$ and $m = 5$, but there is a considerable difference in the observed stability along branches. For the reasonably sharp pulsatile function $P(\theta)$ with $m = 10$ in figure 9a, even the stability properties agree with those for the limiting case in figure 1. In other words, the analytical results, including those on the stability of branches, give the correct description of the properties of the synchronized periodic solutions over the ranges

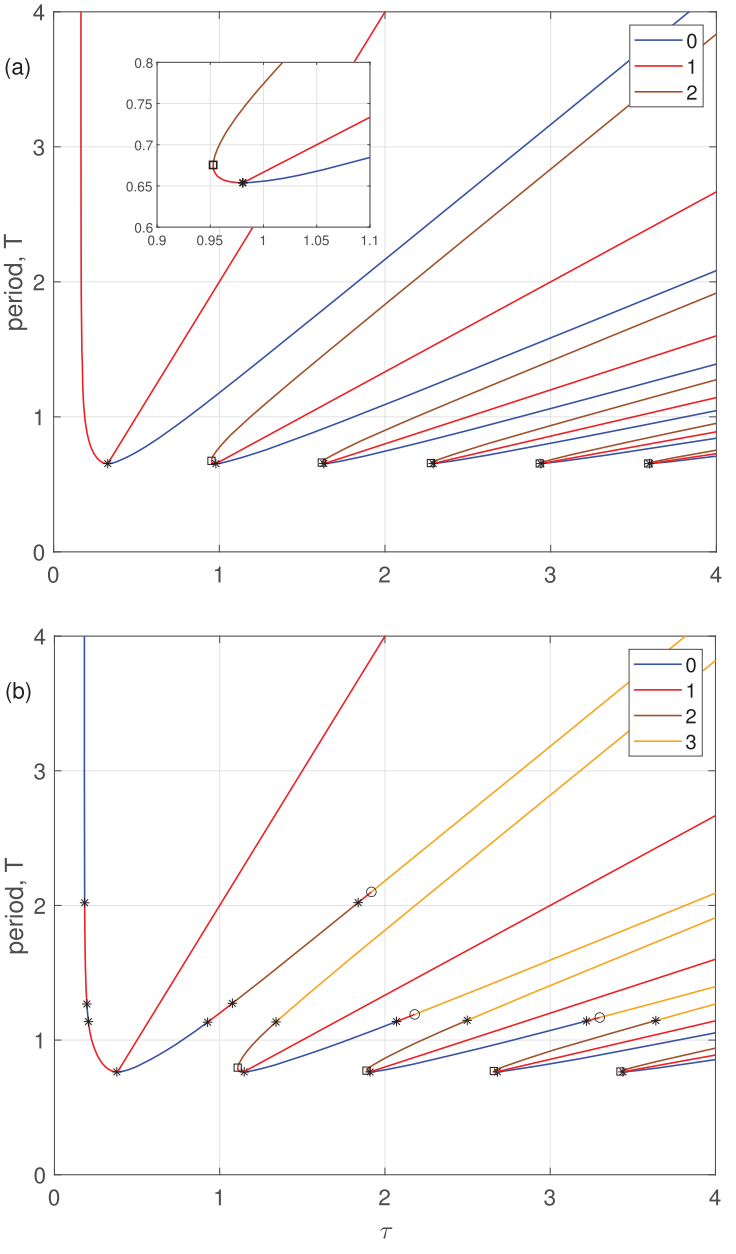

Figure 9. Branches of synchronized and corresponding symmetry-broken periodic solutions of equations (4.2)–(4.3) with $\kappa = 5$ for $m = 10$ in (a) and $m = 5$ in (b). Colour indicates the number of unstable Floquet multipliers, capped at three; saddle-node bifurcations are marked with squares, symmetry-breaking bifurcations with stars and Hopf bifurcations with circles. The inset of (a) is an enlargement of the second branch near the saddle-node and symmetry-breaking bifurcations. Compare with figure 1.

of τ and T that are shown here. When $P(\theta)$ is much less sharp, as in figure 9b for $m = 5$, we find quite a number of additional stability changes, including Hopf bifurcations. While the stability of the branches agrees with that for equations (1.2)–(1.3) sufficiently close to the saddle-node and symmetry-breaking bifurcations, more Floquet multipliers of the synchronized periodic solutions leave or re-enter the unit circle as τ is increased. This observation agrees with that in [8] for the case of a single neuron with delayed self-feedback. For the symmetry-broken synchronized periodic solutions, on the other hand, we do not find additional stability changes.

(b) Alternating solutions

As expected, equations (4.2)–(4.3) also supports alternating periodic solutions of the type studied here; their computed branches are shown in figure 10, again with $\kappa = 5$ and for $m = 10$ in (a) and $m = 5$ in (b). For this type of solution we also find that these branches are very close to and qualitatively as the corresponding ones in figure 5 for the Dirac delta function coupling. Moreover, the stability is still maintained over the same ranges for the 'sharp case' of $P(\theta)$ with $m = 10$, while there are again additional changes of the Floquet multipliers of the alternating periodic solutions when $m = 5$. Importantly, in both cases, except for the branch starting from $\tau = 0$, the branches are born in saddle-node bifurcations and feature subsequent symmetry breaking at their minima.

(i) Symmetry-broken alternating solutions with $\tau = 0$

For $\tau = 0$ the smooth system given by equations (4.2)–(4.3) reduces to a planar system of ODEs, which can be characterized completely. As was the case for the limiting equations (3.26)–(3.27), this smooth equivalent is invariant under both the interchange of neurons 1 and 2, and the reversibility transformation $(t, \theta_1, \theta_2) \mapsto (-t, -\theta_1, -\theta_2)$; the latter is due to the fact that the pulsatile function $P(\theta)$ from equation (4.1) is symmetric about $\theta = \pi$ and about $\theta = 0$. The phase portrait for $\kappa = 5$ and $m = 10$ is shown in figure 11. It features the same equilibria as equations (3.26)–(3.27), but the stable and unstable manifolds of the two saddles $(\theta_1, \theta_2) = (\pi/2, 3\pi/2)$ and $(\theta_1, \theta_2) = (3\pi/2, \pi/2)$ are now not straight lines. While one branch comes from the repellor, or goes to the attractor, the other branches from a pair of homoclinic connections, one to each saddle; compare with figure 6. As figure 11 shows, a region with a family of (neutrally stable) periodic solutions on the torus is bounded by these two homoclinic connections, which also bound the firing lines where, when crossed in the positive direction, the respective neuron fires. A pair of periodic solutions emerges from the unique neutrally stable alternating periodic solutions in figure 11. One such pair is shown, and the period of these periodic solutions increases without bound as they approach the homoclinic connections. Trajectories that are not periodic end up at an equilibrium, namely, the attractor $(\theta_1, \theta_2) = (3\pi/2, 3\pi/2)$ for typical initial conditions. We remark that this mix of 'conservative' and 'dissipative' dynamics in different parts of the phase space is a common property of reversible systems [29]; in particular, it has been discussed previously for a network of three coupled theta neurons [30].

5. Discussion and outlook

We studied perfectly synchronous as well as alternating periodic solutions in a pair of delay-coupled excitatory theta neurons with coupling via a Dirac delta function, given by equations (1.2)–(1.3). This system acts as a 'normal form' for the more general situation of two excitable systems that are mutually coupled subject to a delay—in that it allowed us to determine the existence and stability of these periodic solutions analytically and explicitly. We were also able to explicitly determine the existence and stability of symmetry-broken periodic solutions that bifurcate from the synchronous and alternating ones.

This work can be seen as a natural extension of the case of a single theta neurons with Dirac delta function self-feedback, which we studied in [8]. In fact, the perfectly synchronous solutions can be viewed as arising from self-coupling, and their existence is given by the same expression as for the latter. However, synchronous solutions have different stability properties: they become unstable at the minimum period as a function of the delay τ, rather than at a saddle-node bifurcation as was the case for a single neuron [8]. This change of stability is a symmetry-breaking bifurcation, creating periodic solutions for which the two neurons no longer fire at the same time. Similarly, we considered alternating periodic solutions and showed that they exist with the same period as a perfectly synchronous one, but at a value of τ that is increased (or decreased) by half a period compared to that of the perfectly synchronous solution; the stability properties

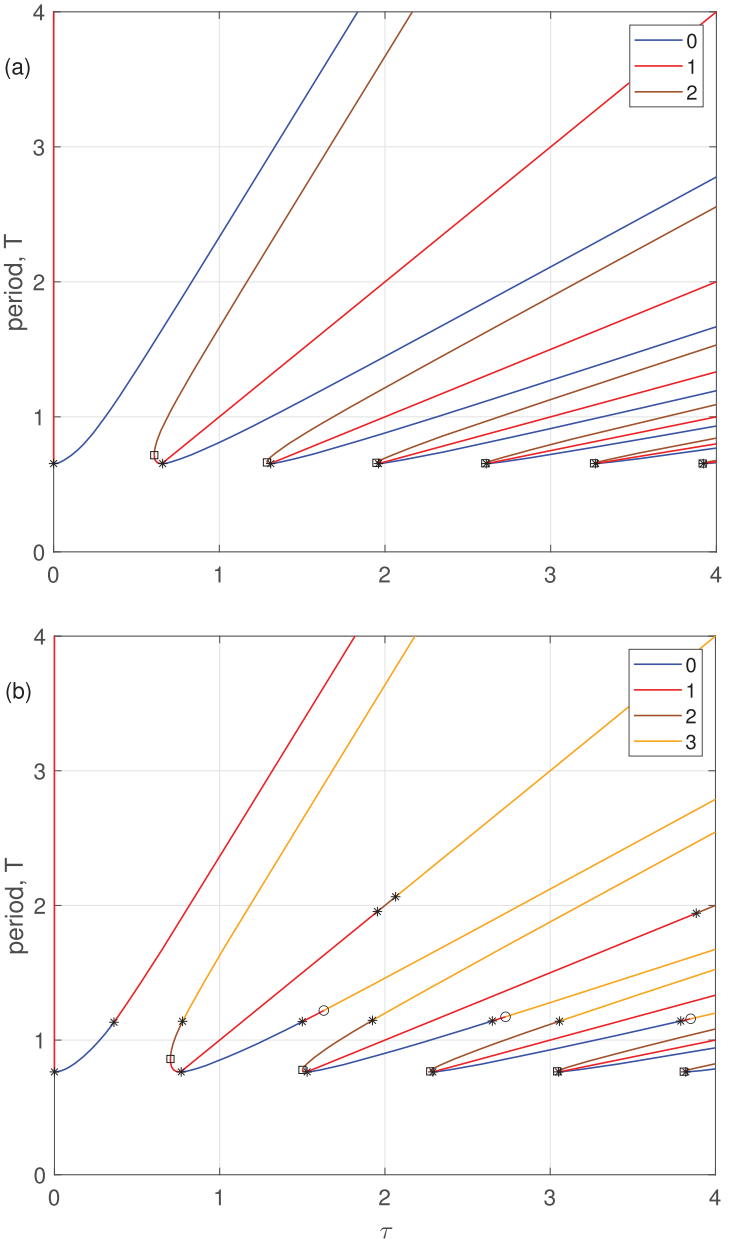

Figure 10. Branches of alternating and corresponding symmetry-broken periodic solutions of equations (4.2)–(4.3) with $\kappa = 5$ for $m = 10$ in (a) and $m = 5$ in (b), shown as in figure 9. Compare with figure 5.

of these two types of periodic solutions are qualitatively the same; in particular, the minima of the period are again symmetry-breaking bifurcations, from which symmetry-broken alternating periodic solutions emerge for which the two neurons no longer fire exactly half a period out of phase with one another. These symmetry-broken solutions exist and can be analysed when $\tau = 0$, and branches for $\tau > 0$ exist due to the reappearance of periodic solutions in DDEs [27].

Overall, there is a clear relationship between the two types of solutions—branches of synchronous periodic solutions given by equation (2.4) and alternating periodic solutions given by equation (3.4). They are interleaved for an increasing number $(n + 1)$ of spikes per period, and can be obtained from one another by the transformation $n \mapsto n + 1/2$. In terms of the delay, this transformation corresponds to replacing τ by $\tau + T/2$, which can be interpreted as 'generated'

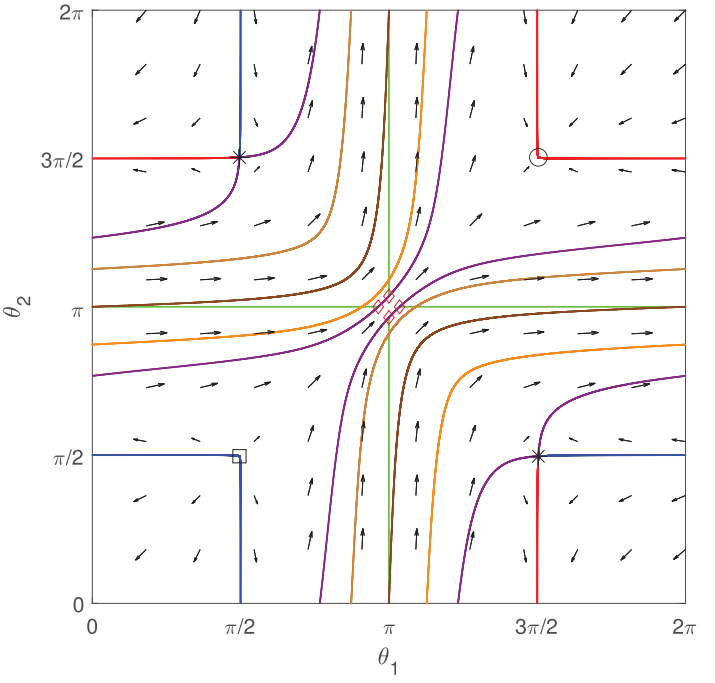

Figure 11. Phase portrait on the square $[0, 2\pi] \times [0, 2\pi]$ of the planar ODE given by equations (4.2)–(4.3) with $\tau = 0$, showing: the repellor (square), the attractor (circle), the two saddle equilibria (crosses) and their invariant manifolds (blue, red and purple curves when forming a homoclinic connection), a pair of symmetry-broken periodic solutions (light brown and orange curves) of the one-parameter family, and the limiting neutrally stable symmetry-broken periodic solution (brown curve). Also shown are the firing lines (green), which are bounded by their intersection points with the homoclinic connections (red diamonds). Here, $\kappa = 5$ and $m = 10$, and the arrows indicate the flow. Compare with figure 6.

by the spatio-temporal symmetry of alternating periodic solutions. This principle applies to the stability calculations as well: by applying the transformation $n \mapsto n + 1/2$, the characteristic equation (3.20) for the alternating solution is identified as that of the synchronous solution in equation (2.15); the same is true for the characteristic equations (A 5) and (A 9) of the respective symmetry-broken periodic solutions.

As a first confirmation that the system is representative in the spirit of a normal form, we also considered equations (4.2)–(4.3) of two theta neurons with smooth, non-impulsive coupling. The resulting smooth DDE was investigated by means of numerical continuation, and this showed that the structure of synchronous and alternating periodic solutions, as well as the respective symmetry-broken ones, is qualitatively the same. Moreover, the stability of these periodic solutions is the same even for coupling via a quite wide pulse; however, when the pulse becomes too wide, there may be additional changes of stability along branches of periodic solutions.

An interesting phenomenon in delay-coupled systems is a phase-flip [31,32], where the phase between oscillators jumps from 0 to π as the delay is varied. This cannot happen in equations (1.2)–(1.3) with Dirac delta function coupling, since a stable branch remains stable as τ is increased. However, a phase-flip may be possible when τ is decreased, or when the coupling is non-instantaneous—as in equations (4.2)–(4.3), where we indeed found additional stability changes for increasing τ for the widest case of the coupling pulse we considered.

We focused here on synchronous and alternating periodic solutions, but there also exist more complicated periodic solutions in equations (1.2)–(1.3), and they may be stable. Figure 12 shows two examples that we found by numerical integration. In (a), the two neurons alternate their firing

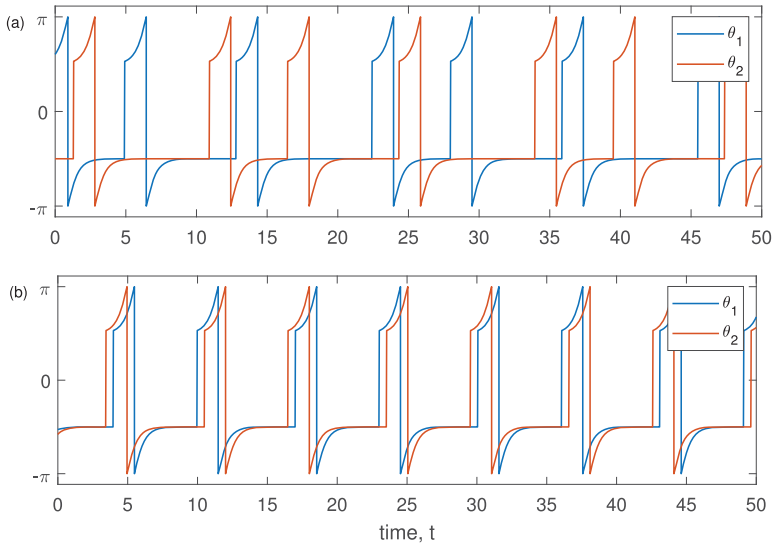

Figure 12. Two stable periodic solutions of equations (1.2)–(1.3) of different types; here, $\kappa = 2.1$ with $\tau = 10$ in (a) and $\tau = 5$ in (b). Compare with figure 3.

times; however, during the period of approximately 23, each neuron fires three times before the pattern repeats. In figure 12b, each neuron fires twice within the period of approximately 12, but without an intervening firing of the other neuron. We remark that a periodic solution with such structure was observed in simulations in [33]. These different types of periodic solutions could be analysed with the methods presented here, although the more firing times there are within the period, the more difficult it is to keep track of them in the calculations required for existence and stability.

While we concentrated here on the excitable case, with $I = -1$, a similar analysis can be done for the free-running case, with $I = 1$ without loss of generality, of two regularly firing theta neurons that are delay-coupled with a Dirac delta function. Two branches of periodic solutions are found, one corresponding to synchronous solutions and the other to alternating solutions. The two branches are connected by symmetry-broken solutions which arise when the period of a solution as a function of the delay is at a maximum or a minimum. These results are presented in [34].

Possible generalizations in the same spirit could include investigating periodic solutions of an excitatory–inhibitory pair of neurons, which may support a PING rhythm [35], or of more complicated networks of three or more theta neurons with Dirac delta function coupling, such as a ring of unidirectionally coupled neurons [36,37], or a chain [38]. Breaking the symmetry between the two neurons may result in interesting behaviour, such as the transients studied in [39].

Data accessibility. This article has no additional data.

Declaration of AI use. We have not used AI-assisted technologies in creating this article.

Authors' contributions. C.R.L.: investigation, methodology, visualization, writing—original draft, writing—review and editing; B.K.: investigation, methodology, visualization, writing—original draft, writing—review and editing.

All authors gave final approval for publication and agreed to be held accountable for the work performed therein.

Conflict of interest declaration. We declare we have no competing interests.

Funding. No funding has been received for this article.

Appendix A. Instability of symmetry-broken periodic solutions

We show here that the symmetry-broken periodic solutions are all unstable, first for those of the synchronous and then for those of the alternating case. The key aspect is that we now have two parameters, γ_1 and γ_2, which are different.

(a) Synchronous case

To find the stability of the symmetry-broken solutions found in §2b, we consider equations (2.9)–(2.10) and evaluate partial derivatives to obtain equations (3.13)–(3.14) as in §3a(iii), but now with

$$\gamma_1 = \frac{\coth^2(\tau - s_i + t_{i-n}) - 1}{[\kappa - \coth(\tau - s_i + t_{i-n})]^2 - 1} = \frac{\coth^2(\tau - (n-\phi)T) - 1}{[\kappa - \coth(\tau - (n-\phi)T)]^2 - 1} \tag{A 1}$$

and

$$\gamma_2 = \frac{\coth^2(\tau - t_i + s_{i-n}) - 1}{[\kappa - \coth(\tau - t_i + s_{i-n})]^2 - 1} = \frac{\coth^2(\tau - (n+\phi)T) - 1}{[\kappa - \coth(\tau - (n+\phi)T)]^2 - 1} \tag{A 2}$$

for the symmetry-broken periodic solution with given ϕ. Again, with $\eta_i = A\lambda^i$ and $\mu_i = B\lambda^i$, equations (3.13)–(3.14) with γ_1 and γ_2 from equations (A 1) to (A 2) can be written as

$$\begin{pmatrix} (1-\gamma_1)\lambda^{i-n} & \gamma_1\lambda^i - \lambda^{i+1} \\ \gamma_2\lambda^i - \lambda^{i+1} & (1-\gamma_2)\lambda^{i-n} \end{pmatrix} \begin{pmatrix} A \\ B \end{pmatrix} = \begin{pmatrix} 0 \\ 0 \end{pmatrix}, \tag{A 3}$$

yielding the characteristic equation

$$\widehat{D}_s(\lambda) := \lambda^{2n}(\lambda - \gamma_1)(\lambda - \gamma_2) - (1-\gamma_1)(1-\gamma_2) = 0 \tag{A 4}$$

for the symmetry-broken synchronous solutions (which gives $D_s(\lambda)$ from equation (2.15) for $\gamma_1 = \gamma_2$). Substituting $T = 2\tau/(2n+1)$ into the definitions of γ_1 and γ_2, and using equation (2.21), one can show that $\gamma_1\gamma_2 = 1$ and $\beta := \gamma_1 + \gamma_2 > 2$. Thus,

$$\widehat{D}_s(\lambda) = \lambda^{2n}(\lambda^2 - \beta\lambda + 1) + \beta - 2,$$

which factorises as $\widehat{D}_s(\lambda) = (\lambda - 1)\widehat{H}_s(\lambda)$, where

$$\widehat{H}_s(\lambda) = \lambda^{2n+1} + (1-\beta)\lambda^{2n} + (2-\beta)\sum_{i=0}^{2n-1}\lambda^i. \tag{A 5}$$

Since $\widehat{H}_s(1) = (2n+1)(2-\beta) < 0$ and $\lim_{\lambda\to\infty}\widehat{H}_s(\lambda) = \infty$, the polynomial $\widehat{H}_s(\lambda)$ has at least one real root greater than 1; thus the symmetry-broken synchronous solutions found in §2b and shown in figure 1 are unstable.

(b) Alternating case for $\tau = 0$

The firing times in equations (3.9)–(3.10) of the alternating periodic solutions with $n = 0$ and $\tau = 0$ are

$$s_{i+1} = t_i + \coth^{-1}[\kappa + \coth(s_i - t_i)] \tag{A 6}$$

and

$$t_{i+1} = s_{i+1} + \coth^{-1}[\kappa + \coth(t_i - s_{i+1})], \tag{A 7}$$

and we write them as

$$R(s_{i+1}, t_i, s_i) = 0$$

and

$$S(t_{i+1}, s_{i+1}, t_i) = 0.$$

Perturbing the firing times as $t_i \to t_i + \eta_i$ and $s_i \to s_i + \mu_i$ and calculating the partial derivatives, we again obtain equations (3.13)–(3.14), but now with

$$\gamma_1 = \frac{1 - \coth^2(t_i - s_i)}{1 - [\kappa - \coth(t_i - s_i)]^2} = \frac{1 - \coth^2((1-\phi)T)}{1 - [\kappa - \coth((1-\phi)T)]^2}$$

and

$$\gamma_2 = \frac{1 - \coth^2(-t_i + s_{i+1})}{1 - [\kappa - \coth(-t_i + s_{i+1})]^2} = \frac{1 - \coth^2(\phi T)}{1 - [\kappa - \coth(\phi T)]^2}.$$

Assuming again that $\eta_i = A\lambda^i$ and $\mu_i = B\lambda^i$ for some constants A, B, we obtain the matrix equation

$$\begin{pmatrix} (1-\gamma_1)\lambda^i & \gamma_1\lambda^i - \lambda^{i+1} \\ \gamma_2\lambda^i - \lambda^{i+1} & (1-\gamma_2)\lambda^{i+1} \end{pmatrix} \begin{pmatrix} A \\ B \end{pmatrix} = \begin{pmatrix} 0 \\ 0 \end{pmatrix},$$

which gives, after multiplication by $-\lambda^{-2i}$ of its determinant, the characteristic equation

$$\lambda^2 - (1 + \gamma_1\gamma_2)\lambda + \gamma_1\gamma_2 = (\lambda - 1)(\lambda - \gamma_1\gamma_2) = 0 \tag{A 8}$$

for the symmetry-broken alternating solutions with $n = 0$. The first factor gives the trivial Floquet multiplier $\lambda = 1$, and the second factor a second Floquet multiplier $\lambda = 1$ because, again, $\gamma_1\gamma_2 = 1$, since equation (3.28) also hold in this case. Thus, these solutions are neutrally stable.

(c) Alternating case for $\tau > 0$

The firing times are given by equations (3.9)–(3.10), and we again linearize around a periodic solution to obtain equations (3.13)–(3.14) with

$$\gamma_1 = \frac{1 - \coth^2(\tau - (n - 1/2 + \phi)T)}{1 - [\kappa - \coth(\tau - (n - 1/2 + \phi)T)]^2}$$

and

$$\gamma_2 = \frac{1 - \coth^2(\tau - (n - 1/2 - \phi)T)}{1 - [\kappa - \coth(\tau - (n - 1/2 - \phi)T)]^2}.$$

Assuming again that $\eta_i = A\lambda^i$ and $\mu_i = B\lambda^i$ for some constants A, B, we obtain

$$\begin{pmatrix} (1-\gamma_1)\lambda^{i-n} & \gamma_1\lambda^i - \lambda^{i+1} \\ \gamma_2\lambda^i - \lambda^{i+1} & (1-\gamma_2)\lambda^{i-n+1} \end{pmatrix} \begin{pmatrix} A \\ B \end{pmatrix} = \begin{pmatrix} 0 \\ 0 \end{pmatrix}.$$

Multiplying the determinant of the matrix above by $-\lambda^{2n-1-2i}$ gives the characteristic equation

$$\widehat{D}_a(\lambda) := \lambda^{2n-1}(\lambda - \gamma_1)(\lambda - \gamma_2) - (1 - \gamma_1)(1 - \gamma_2) = 0$$

for the symmetry-broken alternating solutions with $n \geq 1$. Note that $\widehat{D}_s$ from equation (A 4) is obtained from $\widehat{D}_a(\lambda)$ by the substitution $n \mapsto n + 1/2$. With equation (3.28), and the fact that these solutions have period $T = \tau/n$, it follows again that $\gamma_1\gamma_2 = 1$ and $\beta = \gamma_1 + \gamma_2 > 2$. Paralleling the argument in appendix A(a), we have

$$\widehat{D}_a(\lambda) = \lambda^{2n-1}(\lambda^2 - \beta\lambda + 1) + \beta - 2 = (\lambda - 1)\widehat{H}_a(\lambda)$$

with

$$\widehat{H}_a(\lambda) = \lambda^{2n} + (1 - \beta)\lambda^{2n-1} + (2 - \beta)\sum_{i=0}^{2n-2} \lambda^i, \tag{A 9}$$

which, when substituting $n \mapsto n + 1/2$ here, is exactly $\widehat{H}_s(\lambda)$ from equation (A 5). Hence, by the same argument and with $n \geq 1$ here, $\widehat{H}_a(\lambda)$ has at least one real root greater than 1, and the symmetry-broken alternating solutions found in §3c and shown in figure 5 are also unstable.

Appendix B. Rescaling to $I = -1$

Equation (1.2) with arbitrary negative I takes the form

$$\frac{\mathrm{d}\theta_1}{\mathrm{d}t} = 1 - \cos\theta_1 + (1+\cos\theta_1)\left(-J + \kappa \sum_{i:t-\tau<s_i<t} \delta(t - s_i - \tau)\right),$$

where $J = -I > 0$. With the transformation $V_1 = \tan(\theta_1/2)$, this is equivalent to

$$\frac{\mathrm{d}V_1}{\mathrm{d}t} = V_1^2 - J + \kappa \sum_{i:t-\tau<s_i<t} \delta(t - s_i - \tau). \tag{B 1}$$

The rescaling $\overline{V}_1 = V_1/\sqrt{J}$, $\bar{s}_i = \sqrt{J}s_i$, $\overline{\kappa} = \kappa/\sqrt{J}$, $\bar{t} = \sqrt{J}t$, $\overline{\tau} = \sqrt{J}\tau$ gives

$$J\frac{\mathrm{d}\overline{V}_1}{\mathrm{d}\bar{t}} = J\overline{V}_1^2 - J + \sqrt{J}\overline{\kappa} \sum_{i:\bar{t}-\overline{\tau}<\bar{s}_i<\bar{t}} \delta\left((\bar{t} - \bar{s}_i - \overline{\tau})/\sqrt{J}\right).$$

By using the scaling property of the Dirac delta function and dropping the bars, we obtain equation (B 1) with $J = 1$, which is equivalent to equation (1.2). The result for equation (1.3) is obtained in the same way with $\overline{V}_2 = \tan(\theta_2/2)/\sqrt{J}$, $\bar{t}_i = \sqrt{J}t_i$.

References

1. Izhikevich E. 2007 *Dynamical systems in neuroscience: the geometry of excitability and bursting*. Cambridge, MA: The MIT Press.
2. Krauskopf B, Schneider KR, Sieber J, Wieczorek SM, Wolfrum M. 2003 Excitability and self-pulsations near homoclinic bifurcations in semiconductor laser systems. *Opt. Commun.* **215**, 367–379. (doi:10.1016/S0030-4018(02)02239-3)
3. Ermentrout GB, Kopell N. 1986 Parabolic bursting in an excitable system coupled with a slow oscillation. *SIAM J. Appl. Math.* **46**, 233–253. (doi:10.1137/0146017)
4. Ermentrout B. 1996 Type I membranes, phase resetting curves, and synchrony. *Neural Comput.* **8**, 979–1001. (doi:10.1162/neco.1996.8.5.979)
5. Popovych OV, Hauptmann C, Tass PA. 2006 Control of neuronal synchrony by nonlinear delayed feedback. *Biol. Cybern* **95**, 69–85. (doi:10.1007/s00422-006-0066-8)
6. Laing CR, Longtin A. 2003 Dynamics of deterministic and stochastic paired excitatory-inhibitory delayed feedback. *Neural Comput.* **15**, 2779–2822. (doi:10.1162/089976603322518740)
7. Kelleher B, Bonatto C, Skoda P, Hegarty SP, Huyet G. 2010 Excitation regeneration in delay-coupled oscillators. *Phys. Rev. E* **81**, 036204. (doi:10.1103/PhysRevE.81.036204)
8. Laing CR, Krauskopf B. 2022 Theta neuron subject to delayed feedback: a prototypical model for self-sustained pulsing. *Proc. R. Soc. A* **478**, 20220292. (doi:10.1098/rspa.2022.0292)
9. Garbin B, Javaloyes J, Tissoni G, Barland S. 2015 Topological solitons as addressable phase bits in a driven laser. *Nat. Commun.* **6**, 5915. (doi:10.1038/ncomms6915)
10. Krauskopf B, Walker JJ. 2012 Bifurcation study of a semiconductor laser with saturable absorber and delayed optical feedback. In *Nonlinear laser dynamics* (ed. K Lüdge), pp. 161–181. Weinheim, Germany: Wiley-VCH.
11. Romeira B, Avó R, Figueiredo JML, Barland S, Javaloyes J. 2016 Regenerative memory in time-delayed neuromorphic photonic resonators. *Sci. Rep.* **6**, 19510. (doi:10.1038/srep19510)
12. Terrien S, Krauskopf B, Broderick NGR, Andréoli L, Selmi F, Braive R, Beaudoin G, Sagnes I, Barbay S. 2017 Asymmetric noise sensitivity of pulse trains in an excitable microlaser with delayed optical feedback. *Phys. Rev. A* **96**, 043863. (doi:10.1103/PhysRevA.96.043863)
13. Terrien S, Krauskopf B, Broderick NG, Braive R, Beaudoin G, Sagnes I, Barbay S. 2018 Pulse train interaction and control in a microcavity laser with delayed optical feedback. *Opt. Lett.* **43**, 3013–3016. (doi:10.1364/OL.43.003013)
14. Wedgwood KC, Słowiński P, Manson J, Tsaneva-Atanasova K, Krauskopf B. 2021 Robust spike timing in an excitable cell with delayed feedback. *J. R. Soc. Interface* **18**, 20210029. (doi:10.1098/rsif.2021.0029)

15. Schuster HG, Wagner P. 1989 Mutual entrainment of two limit cycle oscillators with time delayed coupling. *Prog. Theor. Phys.* **81**, 939–945. (doi:10.1143/PTP.81.939)
16. Dodla R, Sen A, Johnston GL. 2004 Phase-locked patterns and amplitude death in a ring of delay-coupled limit cycle oscillators. *Phys. Rev. E* **69**, 056217. (doi:10.1103/PhysRevE.69.056217)
17. Yeung MS, Strogatz SH. 1999 Time delay in the Kuramoto model of coupled oscillators. *Phys. Rev. Lett.* **82**, 648. (doi:10.1103/PhysRevLett.82.648)
18. Dahlem MA, Hiller G, Panchuk A, Schöll E. 2009 Dynamics of delay-coupled excitable neural systems. *Int. J. Bifurcation Chaos* **19**, 745–753. (doi:10.1142/S0218127409023111)
19. Schöll E, Hiller G, Hövel P, Dahlem MA. 2009 Time-delayed feedback in neurosystems. *Phil. Trans. R. Soc. A* **367**, 1079–1096. (doi:10.1098/rsta.2008.0258)
20. Song Y, Xu J. 2012 Inphase and antiphase synchronization in a delay-coupled system with applications to a delay-coupled FitzHugh–Nagumo system. *IEEE Trans. Neural Netw. Learn. Syst.* **23**, 1659–1670.
21. Weicker L, Erneux T, Keuninckx L, Danckaert J. 2014 Analytical and experimental study of two delay-coupled excitable units. *Phys. Rev. E* **89**, 012908. (doi:10.1103/PhysRevE.89.012908)
22. Burić N, Todorović D. 2003 Dynamics of Fitzhugh–Nagumo excitable systems with delayed coupling. *Phys. Rev. E* **67**, 066222.
23. Takamatsu A, Fujii T, Endo I. 2000 Time delay effect in a living coupled oscillator system with the plasmodium of physarum polycephalum. *Phys. Rev. Lett.* **85**, 2026. (doi:10.1103/PhysRevLett.85.2026)
24. Klinshov V, Nekorkin V. 2011 Synchronization of time-delay coupled pulse oscillators. *Chaos Solitons Fractals* **44**, 98–107. (doi:10.1016/j.chaos.2010.12.007)
25. Li P, Lin W, Efstathiou K. 2017 Isochronous dynamics in pulse coupled oscillator networks with delay. *Chaos* **27**, 053103. (doi:10.1063/1.4982794)
26. Golubitsky M, Stewart I, Schaeffer DG. 2012 *Singularities and groups in bifurcation theory: volume II*, vol. 69. New York: Springer Science & Business Media.
27. Yanchuk S, Perlikowski P. 2009 Delay and periodicity. *Phys. Rev. E* **79**, 046221. (doi:10.1103/PhysRevE.79.046221)
28. Sieber J, Engelborghs K, Luzyanina T, Samaey G, Roose D. 2015 *DDE-BIFTOOL Manual — Bifurcation analysis of delay differential equations*. (http://arxiv.org/abs/1406.7144). Available at https://sourceforge.net/projects/ddebiftool.
29. Roberts JA, Quispel G. 1992 Chaos and time-reversal symmetry. Order and chaos in reversible dynamical systems. *Phys. Rep.* **216**, 63–177. (doi:10.1016/0370-1573(92)90163-T)
30. Laing CR. 2018 Chaos in small networks of theta neurons. *Chaos* **28**, 073101. (doi:10.1063/1.5028515)
31. Prasad A, Kurths J, Dana SK, Ramaswamy R. 2006 Phase-flip bifurcation induced by time delay. *Phys. Rev. E* **74**, 035204. (doi:10.1103/PhysRevE.74.035204)
32. Adhikari BM, Prasad A, Dhamala M. 2011 Time-delay-induced phase-transition to synchrony in coupled bursting neurons. *Chaos* **21**, 023116. (doi:10.1063/1.3584822)
33. Horvath V, Gentili PL, Vanag VK, Epstein IR. 2012 Pulse-coupled chemical oscillators with time delay. *Angew. Chem.* **124**, 6984–6987. (doi:10.1002/ange.201201962)
34. Laing CR. 2024 Periodic solutions for a pair of delay-coupled active theta neurons. *ANZIAM J.* **67**, e11. (doi:10.1017/S1446181124000282)
35. Börgers C, Kopell N. 2005 Effects of noisy drive on rhythms in networks of excitatory and inhibitory neurons. *Neural Comput.* **17**, 557–608. (doi:10.1162/0899766053019908)
36. Klinshov V, Lücken L, Yanchuk S, Nekorkin V. 2018 Multi-jittering instability in oscillatory systems with pulse coupling. In *Chaotic, fractional, and complex dynamics: new insights and perspectives* (eds. M Edelman, EEN Macau, MAF Sanjuan), pp. 261–285. New York, NY: Springer.
37. Perlikowski P, Yanchuk S, Popovych OV, Tass PA. 2010 Periodic patterns in a ring of delay-coupled oscillators. *Phys. Rev. E* **82**, 036208. (doi:10.1103/PhysRevE.82.036208)
38. Ermentrout G, Kopell N. 1990 Oscillator death in systems of coupled neural oscillators. *SIAM J. Appl. Math.* **50**, 125–146. (doi:10.1137/0150009)
39. Ermentrout GB, Rinzel J. 1996 Reflected waves in an inhomogeneous excitable medium. *SIAM J. Appl. Math.* **56**, 1107–1128. (doi:10.1137/S0036139994276793)